“Monitoring soil salinity using time-lapse electromagnetic conductivity imaging” - authors’ responses to suggestions and comments made by Topical Editor Jan Vanderborght

Dear topical editor Jan Vanderborght,

We sincerely appreciate and thank your constructive comments on our manuscript. We have revised the manuscript according to your suggestions and comments. We hope that the revised version of the manuscript properly addresses your concerns.

Our answers are placed in blue below each of your comments. The changes to the manuscript, arising from your comments, are written in grey.

Sincerely,
Mohammad Farzamian on behalf of all authors

Authors responses to topical editor Jan Vanderborght's comments

Comments to the Author:

Dear,

I agree with your replies to the comments of the reviewers.

However, I have two main additional comments.

We thank you very much for pointing out these two very relevant and constructive questions.

The first is on the statistical evaluation of agreement between the measured and EMI derived ECe's. This was to my opinion not clearly described and I propose including the equations that were used to calculate the RMSEs, R2 and other indices. The reason for including these is that there is an ambiguity about what you use as predicted value when you calculate these indices. The ECe that you obtained from the EMI estimated sigma and a regression equation, or the prediction of the measurement from a regression between the EMI derived ECe and the measured ECe?

We have added a table with the equations used for calculating the statistical indicators, and also revised section 2.4 as follows:

Old version (line 135–in section 2.4)

"In the present study, the regional calibration was used to predict EC_e from time-lapse EMCI. The predicted EC_e and EC_emeasured from soil samples, collected from July 2017 to October 2018, were used to validate the regional calibration as anindependent test set.Its prediction ability was evaluated by calculating the root mean square error (RMSE), the coefficient ofdetermination (R^2) between the measured and predicted EC_e, the Lin's concordance correlation coefficient (CCC), and the mean error (ME).The RMSE is the square root of the mean of the squared differences between the measured and predicted EC_e, indicating how concentrated the data is around the linear regression. In this study we used two degrees of freedom for a more robust calculation of RMSE. The coefficient of determination (R^2) indicates how well the predicted EC_e approximate the measured EC_e. When this is 1, it means the predictions coincide with the measurements. Lin's CCC measures the agreement between the measured and predicted EC_e evaluating how close the linear regression is to the 1:1 relationship and ranges from −1 to 1, with perfect agreement at 1 (Lin, 1989). ME is the mean of all differences between the measured and predicted EC_e and evaluates whether the linear regression consistently over- and underestimates the predicted ECe. Therefore, the prediction is more precise and less biased when the RMSE and the ME are closer to zero."

New version

"In the present study, the regional calibration was used to predictEC_e from time-lapse EMCI (pEC_e). The predicted EC_e and EC_emeasured from soil samples (mEC_e), collected at the same time as the EMI surveys, were used as an independent data set for the validation of the regional calibration. The validation was performed by calculating the root mean square error (RMSE), the coefficient of determination (R^2) between the measured and predicted EC_e, the Lin's concordance correlation coefficient (CCC), and the mean error (ME). Description of these statistical indicators and the equations used to calculate them are shown in Table 1. Calculations were done using global data, and also using data discriminated by date of measurement (in this case we considered dates when measurements were done at the four locations – January, June and October 2018), depth of measurement and location."

Table 1 – Description and equations of the statistical indicators used to evaluate the prediction ability of the regional calibration in this work.

Statistics	Equation[1]	Description
Root mean square error (RMSE)	$\mathrm{RMSE} = \sqrt{\frac{\sum_{i=1}^{n}(\mathrm{mEC}_{e_i} - \mathrm{pEC}_{e_i})^2}{n-2}}$	Evaluates matching between measured and predicted data. When it is zero, it indicates perfect matching between measured and predicted data.
Mean error (ME)	$\mathrm{ME} = \frac{\sum_{i=1}^{n}(\mathrm{mEC}_{e_i} - \mathrm{pEC}_{e_i})}{n}$	Evaluates whether the predicted data are over- or underestimated. A negative value means overestimation, a positive value means underestimation.
Lin's concordance correlation coefficient (Lin's CCC)	$\mathrm{Lin's\ CCC} = \frac{2s_{\mathrm{mEC}_e - \mathrm{pEC}_e}}{s^2_{\mathrm{mEC}_e} + s^2_{\mathrm{pEC}_e} + (\overline{\mathrm{mEC}_{e_i}} - \overline{\mathrm{pEC}_{e_i}})^2}$	Evaluates agreement between measured and predicted data. Ranges from -1 to 1. When it is 1, it indicates perfect agreement between measured and predicted data (Lin, 1989).
Coefficient of determination (R^2)	$R^2 = \left(\frac{\sum_{i=1}^{n}(\mathrm{mEC}_{e_i} - \overline{\mathrm{mEC}_{e_i}})(\mathrm{pEC}_{e_i} - \overline{\mathrm{pEC}_{e_i}})}{\sqrt{\sum_{i=1}^{n}(\mathrm{mEC}_{e_i} - \overline{\mathrm{mEC}_{e_i}})^2}\sqrt{\sum_{i=1}^{n}(\mathrm{pEC}_{e_i} - \overline{\mathrm{pEC}_{e_i}})^2}} \right)^2$	Indicates the degree of linearity between predicted and measured data. Ranges from 0 to 1. Above 0.5 is considered satisfactory.

[1]n is the total number of data; mEC_e is measured EC_e; pEC_e is predicted EC_e; the upper bar represents the mean of the indicated data.

The second main (and more critical) comment is that you do not address the real issue of this paper, namely, can you use EMI to MONITOR ECe, i.e. to evaluate whether it changes over time. You are only discussing that you observe changes over time. But, are the changes you observe in the soil sample measurements consistent with the changes that you observe in the EMI measurements? You do not address this issue and I think this is crucial. A negative answer to this question will not lead to a rejection of your paper. But, you need to answer this question using appropriate statistical analyses. If this question is not answered appropriately, the work that you present is not meeting the objectives that are suggested in the title, the introduction and the conclusion and can therefore not be accepted.

Relatively to the second question, we added specific statistical analyses to investigate the prediction ability of the calibration in time and at different locations and depths to address the editor´s concern. The new analysis shows that the prediction ability of the regional calibration does not vary significantly over time. However, the changes in predicted EC_e are not completely consistent with the changes in measured EC_e. This is partly due todifferent spatial and temporal variations of other soil properties at each location which influence spatio-temporal variations of σ differently and limit inferring soil salinity changes using time-lapse EMCI data and regional calibration, as pointed out by the editor.On the other hand, the regional calibration is more influenced by the spatial variability of EC_e at location 4 which also limits a quantitative investigation of soil salinity changes from time-lapse EMI surveys at other locations.

The new statistical analyses added to the revised version of the manuscript suggests that the regional calibration approach still stands as an expeditious method to predict soil salinity from EMI in the study area (any new locations in the study area), since the prediction ability of the regional calibration has not been changed significantly. However, a location-specific calibration is required for a more precise assessment of soil salinity changes at each location.We also detected an outlier (in the lower subsoil at location 2), and took it out – this changed slightly the results presented for the global statistical indicators. We revised the text and Fig. 4 in this light and we propose a new title for the paper which may better represent the results of this study.

Old version (Title)

"Monitoring soil salinity using time-lapse electromagnetic conductivity imaging"

New version

"Assessing soil salinity dynamics using time-lapse electromagnetic conductivity imaging"

Old version (line 23–in Abstract)

"This study aims to evaluate the potential of time-lapse EMCI and the regional calibration to predict the spatiotemporal variability of soil salinity in the study area. The results showed that EC_e was satisfactorily predicted, with a root mean square error (RMSE) of 3.22 dS m^{-1} in a range of 52.35 dS m^{-1} and a coefficient of determination (R2) of 0.89. Results also showed strong concordance with a Lin's concordance correlation coefficient (CCC) of 0.93, although, EC_e was slightly overestimated with a mean error (ME) of −1.30 dS m^{-1}. Soil salinity maps for each location revealed salinity fluctuations related to the input of salts and water either through irrigation, precipitation or groundwater level and salinity. Time-lapse EMCI has proven to be a valid methodology for evaluating the risk of soil salinization, and can further support the evaluation and adoption of proper agricultural management strategies, especially in irrigated areas, where continuous monitoring of soil salinity dynamics is required."

New version

"Using time-lapse EMCI data, this study aims (1) to evaluate the ability of the regional calibration to predict soil salinity, and (2) to perform a preliminary qualitative analysis of soil salinity dynamics in the study area. The validation analysis showed that

$EC_e$was predicted with a root mean square error (RMSE) of 3.14 dS m^{-1} in a range of 52.35 dS m^{-1}, slightly overestimated (−1.23 dS m^{-1}), with a strong Lin's concordance correlation coefficient (CCC) of 0.94 and high linearity between measured and predicted data (R^2 = 0.90). It was also observed that the prediction ability of the regional calibration is more influenced by spatial variability of data than temporal variability of data. Soil salinity cross sections were generated for each date and location of data collection, revealing qualitative salinity fluctuations related to the input of salts and water either through irrigation, precipitation, and level and salinity of groundwater. Time-lapse EMCI is developing into a valid methodology for evaluating the risk of soil salinization, so it can further support the evaluation and adoption of proper agricultural management strategies, especially in irrigated areas, where continuous monitoring of soil salinity dynamics is required."

Old version (line 59 - in section 2 - Introduction)

"When repeated over a period of time, EMCI of a study area is called time-lapse EMCI, and can be used to monitor the dynamics of soil salinity and other soil properties. Time-lapse EMCI has been successfully used to monitor soil water content (Huang et al., 2017; 2018; Moghadas et al., 2017) although, to our knowledge, its potential for monitoring soil salinity has not been previously investigated.

This study aims to evaluate the potential of time-lapse EMCI and a previously developed regional calibration to predict the spatiotemporal variability of soil salinity, and to monitor and evaluate soil salinity dynamics in the study area. For this purpose, EMI measurements and soil sampling were carried out between May 2017 and October 2018 at four locations with different salinity levels across the study area. EMI measurements were performed with a single-coil instrument (EM38), collecting EC_a data in the horizontal and vertical orientations and at two heights, and then inverted to obtain EMCI, which provides a vertical distribution of σ. Finally, σ was converted to EC_e through the previously developed regional calibration. Soil samples were collected along the EMI transects, and used for laboratory determination of EC_e. These data were used as an independent test set to evaluate the ability of the regional calibration to predict the spatiotemporal variability of soil salinity, and to generate soil salinity maps for each date of data collection."

New version

"When repeated over a period of time at the same place, EMCI becomes time-lapse EMCI and can be used to investigate the dynamics of soil properties such as soil water content (Huang et al., 2017; 2018; Moghadas et al., 2017). Using time-lapse EMCI data, this study aims (1) to evaluate the ability of a previously developed regional calibration to predict soil salinity, and (2) to perform a preliminary qualitative analysis of soil salinity dynamics in the study area. For this purpose, EMI measurements and soil sampling were carried out between May 2017 and October 2018 at four locations with different salinity levels across the study area. EMI measurements were performed with a single-coil instrument (EM38), collecting EC_a data in the horizontal and vertical orientations and at two heights, and then inverted to obtain EMCI, which provides a vertical distribution of σ. Finally, σ was converted to EC_e using the previously developed regional calibration. Soil samples were collected along the EMI transects, and used for laboratory determination of EC_e. These data were used as an independent dataset to evaluate the ability of the regional calibration to predict soil salinity, and to generate soil salinity cross sections for each date of data collection."

Old version (line 130 – in section 2.4)

"However, the regional calibration can be used at any new location in the study area, within the range of measured EC_e, which makes it highly suitable for mapping and monitoring salinity in the study area."

New version

"However, the regional calibration can be used at any new location in the study area, within the range of measured EC_e, which makes it highly suitable for mapping salinity in the study area."

Old version (line 169–in section 4.2)

"Figure 5 shows EC_e predicted with the regional calibration versus the measured EC_e and the 1:1 line, with points identified in terms of date of measurement (Fig. 4a) and depth of measurement (Fig. 4b). Prediction of EC_e with the regional calibration using data collected from July 2017 to October 2018 resulted in a RMSE of 3.22 dS m^{-1} and R2 of 0.89, which indicates satisfactory prediction ability, given the large range of EC_e (52.35 dS m^{-1}). The high global Lin's CCC of 0.93 shows accord between measured and predicted ECe. The ME is −1.30 dS m^{-1}, indicating that the regional calibration globally overestimates EC_e. Figure 4a and Fig. 4b show that the points are generally scattered around the 1:1 line and it is not possible to identify variations depending on the date or depth of the measurement. In order to analyze the prediction ability at each location, Fig. 4c and Fig. 4d display an enlargement of the lower left part of the previous figures, displaying ECe values below 15 dS m^{-1}. Figure 4c and Fig. 4d show differences in the prediction ability according to the location, namely at locations 2 and 3, where EC_e is generally overestimated. At location 2, EC_e is more overestimated in deeper soil layers (Fig. 4d) which is likely due to a previously identified influence of clay content that consistently increases with depth at this location, while it is rather uniform or declines with depth at the other locations (Farzamian et al., 2019).

The validation procedure used in this study gives lower prediction ability for the regional calibration than the previously obtained with the leave-one-out-cross-validation (see section 2.4). This can be justified because the test set is completely independent from the dataset used to develop the calibration. Furthermore, this test set is composed of measurements collected over a wider period of time (18 months). During this period, soil properties, which are also known to influence σ, such as θ, change (as shown in Fig. 3), which introduces larger variability in the measurements. However, and given the large range of EC_e (52.35 dS m^{-1}), a RMSE of 3.22 dS m^{-1} is acceptable for this type of non-invasive and indirect method. The regional calibration could be further developed by including measurements taken over a longer period of time in the calibration process, in order to include a wider range of variation of soil properties.

New version

"For a specific evaluation of the prediction ability of the regional calibration, Table 2 shows the statistical indicators obtained using global data, i.e., data collected at all locations, from July 2017 to October 2018, and the statistical indicators for each date, soil depth, and location. The validation of the regional calibration using global data resulted in a RMSE of 3.14 dS m^{-1} and R^2 of 0.90, which indicates satisfactory prediction ability, given the large range of EC_e (52.35 dS m^{-1}). The high global Lin's CCC of 0.94 shows agreement between measured and predicted EC_e. The ME is −1.23 dS m^{-1}, indicating that the regional calibration generally overestimates EC_e. The statistical indicators discriminated by date of measurement (in this case we considered only the dates when measurements were done at the four locations – January, June and October 2018), shown in Table 2, also indicate that the prediction ability doesn't vary significantly when comparing the statistical indicators of the three dates. The validation procedure used in this study gives slightly lower prediction ability for the regional calibration than the previously obtained with the leave-one-out-cross-validation (see section 2.4). This is expected as thisdataset is completely independent from the dataset used to develop the calibration and was collected over a wider period of time (18 months). During this period, soil properties, which are also known to influence σ, such as temperature and θ, change, which introduces larger variability in data.

In terms of the influence of depth of measurement, prediction ability improves with depth, being weak at top soil, and very good from the subsurface to the lower subsoil. We attribute the weak prediction ability at top soil to the smaller range of EC_e variability (0.35–5.17 dS m^{-1}) and to the larger variability of other soil properties (e.g. θ and temperature), which are due to

different irrigation schemes and cultivated crops at each location. In terms of the influence of each location, prediction ability varies considerably. At location 1, prediction ability is very poor, with a low R^2, which means the degree of linearity between predicted and measured data is low, and a high RMSE within the considered range of EC_e. At this location, however, the soil is non-saline and the range of EC_e, is very small (0.35–1.89 dS m^{-1}) and thus other soil properties such as θ and clay content have larger impact on spatiotemporal variability of σ. At locations 2, 3 and 4, prediction ability of the regional calibration is acceptable at the former two, and good at the latter. We can analyse better these results when observing Fig. 5, which shows EC_e predicted with the regional calibration versus the measured EC_e and the 1:1 line, with data identified in terms of date of measurement (Fig. 5a) and depth of measurement (Fig. 5b). Fig. 5c and Fig. 5d display an enlargement of the lower left part of the previous figures, displaying EC_e values below 15 dS m −1, and data relative to locations 1, 2 and 3 at different depths. At location 2, EC_e is more overestimated in deeper soil layers (Fig. 4d) which is likely due to the clay content that consistently increases with depth at this location, while it is rather uniform or declines with depth at the other locations (Farzamian et al., 2019). This is probably also the main reason for the very low Lin's CCC at this location. At location 3, EC_e is also overestimated (Fig. 5d), most likely due to the influence of θ and cation exchange capacity (Paz et al., 2019a) which are higher on average compared to locations 2 and 4. Finally, the EC_e ranges of location 4 and of the lower subsoil are similar to the EC_e range of global data, showing dominance of location 4 and of lower subsoil data on the calibration.

These results show that spatial variability of data has a much stronger influence on the prediction ability of the regional calibration, than temporal variability of data. This spatial sensitivity of the regional calibration can be improved by studying new locations across the study area to include a wider variability of soil properties and ranges of EC_e in the calibration process. On the other hand, longer observation periods andmore frequent EMI surveying and soil sampling, as well as monitoring of other soil dynamic properties that influence σ (i.e. θ, soil temperature, level and salinity of groundwater) and finding ways to quantitatively account for their impact on time-lapse EMCIs,can improve the temporal sensitivity of regional calibration.

Table 2 – RMSE, ME, Lin's CCC, R2, minimum, maximum and range of ECe, and the number of data used to calculate these statistical indicators, discriminated in terms of global, date of measurement, depth of measurement and location.

	RMSE (dS m^{-1})	ME (dS m^{-1})	Lin's CCC	R^2	EC_e min (dS m^{-1})	EC_e max (dS m^{-1})	EC_e range (dS m^{-1})	Number of data
Global	3.14	−1.23	0.94	0.90	0.35	52.70	52.35	103
Jan 2018	2.79	−1.33	0.96	0.93	0.59	35.90	35.31	30
Jun 2018	4.27	−0.08	0.94	0.94	0.35	52.70	52.35	20
Oct 2018	3.11	−0.71	0.96	0.93	0.44	42.50	42.06	19
0–0.3 m	1.79	−0.39	0.39	0.19	0.35	5.17	4.82	21
0.3–0.6 m	1.74	−0.34	0.78	0.67	0.42	8.86	8.44	21
0.6–0.9 m	2.40	−1.61	0.89	0.91	0.42	16.72	16.30	21

0.9–1.2 m	4.77	−3.25	0.89	0.89	0.49	32.10	31.61	21
1.2–1.5 m	4.71	−0.87	0.95	0.93	0.60	52.70	52.10	20
Location 1	1.23	−0.59	−0.05	0.02	0.35	1.89	1.54	35
Location 2	3.22	−2.40	0.23	0.56	0.91	3.86	2.95	24
Location 3	3.88	−2.56	0.44	0.47	1.98	9.85	7.87	24
Location 4	4.63	0.65	0.94	0.90	2.33	52.70	50.37	20

Old version (Figure 4)

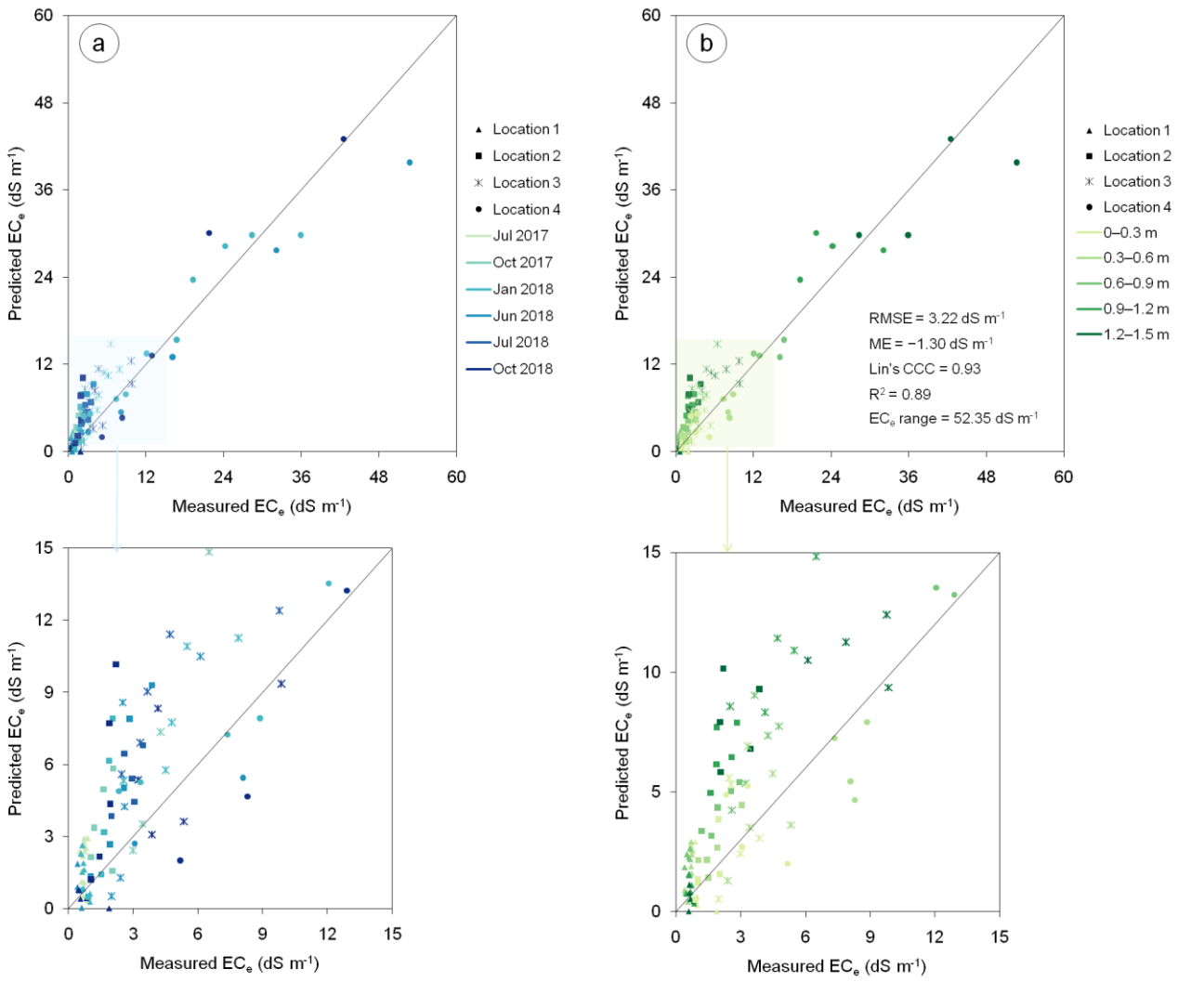

New version (Figure 5)

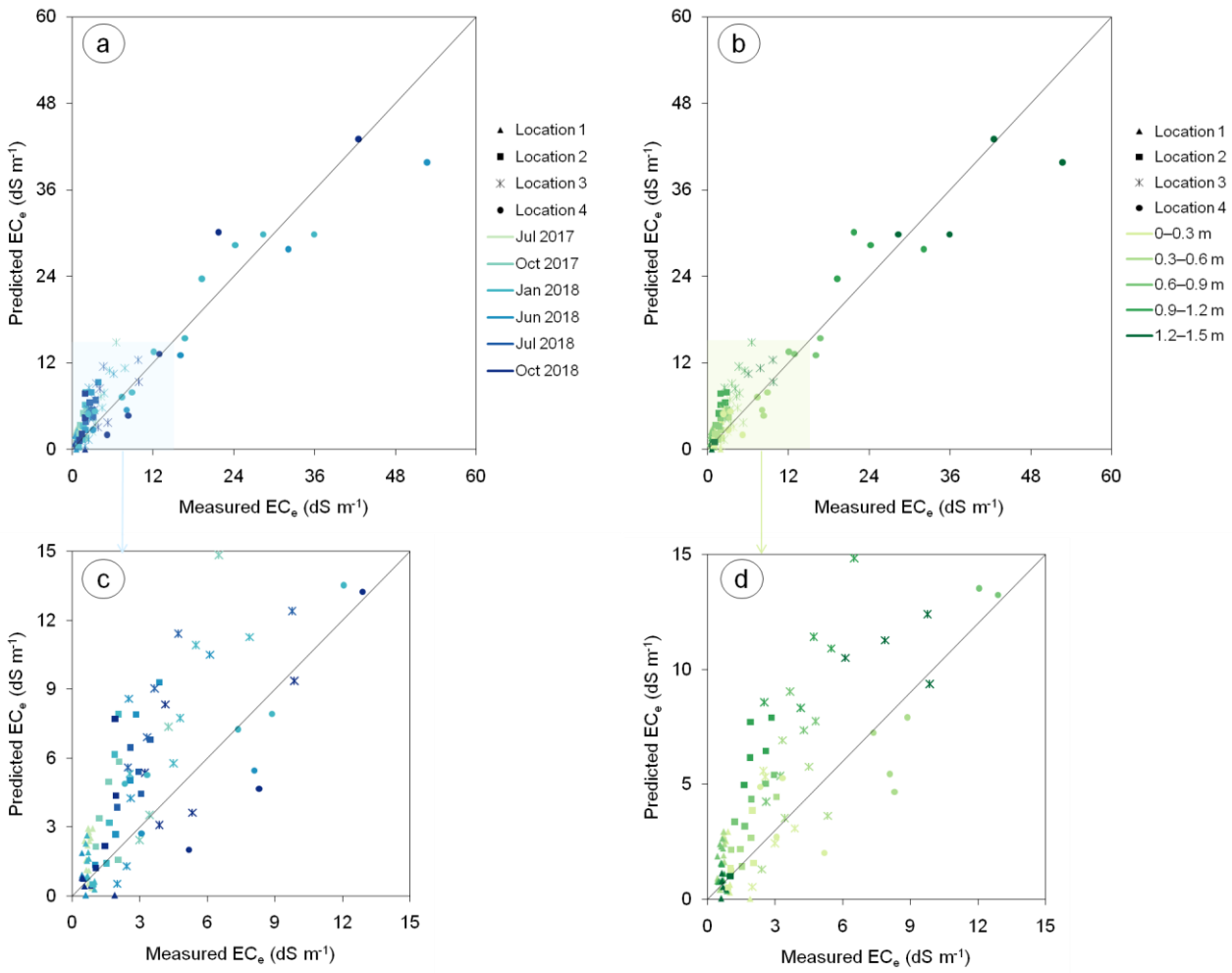

Old version (line 195 - title of section 4.3)

"4.3 Spatiotemporal mapping of soil salinity from time-lapse EMCI"

New version (already comprising suggestions from referees)

"4.4 Generation of soil salinity cross sections from time-lapse EMCI"

Old version (line 236 - section 5 - Conclusion)

"In this study, EMI and soil sampling data collected between May 2017 and October 2018 were used, together with a previously developed regional calibration, to predict the spatiotemporal variability of soil salinity. This procedure allowed further validation of the regional calibration with an independent test set. This validation resulted in lower prediction ability than that previously resulting from cross-validation, not only because the test set was independent, but also because it was collected over a wider period of time, during which the variation of soil properties is larger. The validation used in this study resulted in a RMSE of 3.22 dS m^{-1}, which is acceptable given the large range of EC_e (52.35 dS m^{-1}). As a result, the regional calibration approach still stands as an expeditious method to predict soil salinity in the study area over time. The regional calibration could be further developed by studying new locations across the study area in order to include a wider range of variation of soil properties. Also, a longer period of observation could further improve the regional calibration. Furthermore, the influence of static soil properties (i.e., that do not vary in time), such as clay content, could be tackled with the use of maps of the variation of soil salinity between two consecutive dates, which allows removing the static effect in the EMCIs.

Relatively to the inversion process, in the absence of a time-lapse inversion algorithm, EC_a data was inverted independently. This method can distort the inversion results, since the reference model and a priori information are not considered. Further research involves time-lapse inversion algorithms that are being developed to invert data collected with EMI sensors, which can generate EMCIs of higher precision.

The methodology used in this study allowed the creation of soil salinity maps displaying the spatiotemporal patterns of soil salinity at four locations in the study area. The salinity maps reveal fluctuations in time related to the input of salts and water either through irrigation, precipitation or groundwater level and salinity. In a regional perspective, soil salinity dynamics in the study area may be explained by a combination of spatial distribution of the marine fraction of soil, with irrigation practices in the study area and saline groundwater in the southern part. Continuous monitoring of salinity in the study area, along with detailed data collection about irrigation, precipitation, evapotranspiration, leaching, groundwater flow, and tides, can be helpful to further study soil salinity dynamics.

Time-lapse EMCI has proven to be a valid methodology for evaluating risk of soil salinization, and can further support the evaluation and adoption of proper agricultural management strategies, especially in irrigated areas, where continuous monitoring of soil salinity dynamics is required."

New version (already comprising suggestions from referees)

"In this study, EMI and soil sampling data collected between May 2017 and October 2018 were used, together with a previously developed regional calibration, to predict soil salinity. This procedure allowed further validation of the regional calibration with an independent dataset and a preliminary qualitative analysis of soil salinity dynamics in the study area. Based on the comprehensive analysis of the statistical indicators obtained from the validation process, and the obtained soil salinity cross sections, the following main conclusions can be drawn:

1. The validation performed in this study resulted in a RMSE of 3.14 dS m^{-1}, which is acceptable given the large range of EC_e (52.35 dS m^{-1}). This validation resulted in lower prediction ability than that previously resulting from cross-validation. This is because the test set was independent, and also because it was collected over a wider period of time,

with a larger variation of soil properties. In addition, prediction ability of the regional calibration does not vary significantly over time. As a result, the regional calibration approach still stands as an expeditious method to predict soil salinity from EMI surveys at any new location in the study area. However, prediction ability of the regional calibration in assessing variability of soil salinity at different locations and depths varies significantly due to variability of soil properties at each location and depth. Our investigation shows that significantly larger variations of EC_e and σ at location 4 dominated the regional regression calibration, suggesting a good prediction ability of the regional calibration in the south of the study area and close to location 4 where the soil salinization is of major concern and can compromise agricultural activity.

2. The methodology used in this study allowed the generation of soil salinity cross sections displaying the patterns of soil salinity at different dates, at four locations in the study area. The salinity cross sections show a qualitative response of soil salinity to the input of salts and water either through irrigation, precipitation or level and salinity of groundwater. In a regional perspective, soil salinity dynamics in the study area may be preliminarily explained by a combination of spatial distribution of the marine fraction of soil, with irrigation practices in the study area and saline groundwater in the southern part.

Application of time-lapse EMCI and calibration for assessing soil salinity dynamicsis a developing methodology that can further support the evaluation and adoption of proper agricultural management strategies in irrigated regions. Some aspects can and will be addressed in future studies so to improve its performance. From this study, we identify some of these aspects. First, relatively to the inversion process, and in the absence of a time-lapse inversion algorithm, EC_a data was inverted independently. This method can distort the inversion results, since the reference model and a priori information are not considered. Further research involves time-lapse inversion algorithms that are being developed to invert data collected with EMI sensors, which can generate EMCIs of higher precision. Secondly, the influence of static soil properties (i.e., that do not vary in time), such as clay content and cation exchange capacity, could be tackled with the use of cross sections of the variation of soil salinity between two consecutive dates, which allows removing the static effect from the time-lapseEMCIs. Finally, temporal soil salinity assessment can be optimized by quantitatively taking into account the influence of soil dynamic properties on the time-lapse EMCIs. Specifically, in Lezíria, regional calibrations can be improved by studying new locations across the study area for a longer period of time with more frequent surveying and sampling, and also by including new parameters, such as θ, soil temperature, level and salinity of groundwater. However, the temporal variations of these properties are connected to location specific conditions. For instance, θ can vary significantly in the study area, particularly in the root zone, due to different irrigation practices, rootup take of different crops, and fluctuation of groundwater level. These facts highlight the necessity of using location-specific calibrations for a more precise assessment of soil salinity changes at each location."

Detailed comments:

Ln 15: You could maybe include here why the soil faces a risk of salinization in this area.

The soil faces the risk of salinization due to the influence of the ocean tides in groundwater in the southern part of the peninsula. Irrigation can also represent a salinization risk at the northern locations. Climate change is likely to aggravate these risks through the rise of sea water level (resulting in the rise of the saline groundwater and increased salinity of the irrigation water, which is collected from the river, upstream of the estuary), the increase in temperature and decrease in rainfall, which can lead to the accumulations of salts in the soil profile.

The proposed change is presented below.

Old version (line 14 – in Abstract)

"Lezíria Grande of Vila Franca de Xira, located in Portugal, is an important agricultural system where soil faces the risk of salinization, being thus prone to desertification and land abandonment."

New version

"Lezíria Grande of Vila Franca de Xira, located in Portugal, is an important agricultural system where soil faces the risk of salinization due to climate change, as the level and salinity of groundwater are likely to increase, as a result of the rise of the sea water level and consequently of the estuary. These changes can also affect the salinity of the irrigation water which is collected upstream of the estuary."

To avoid confusion, I propose to use the same units for ECa, sigma, and ECe.

In fact, there was a lapse in the units of EC_a, thank you for noticing it. It should be in mS m^{-1}. The manuscript will be corrected accordingly.

Relatively to EC_e and σ, we maintained the same units, since the calibration equation that is a substantial part of this paper was parameterized for EC_e in dS m^{-1} and σ in mS m^{-1}.

Ln 23: 'This study aims to evaluate the potential of time-lapse EMCI and the regional calibration to predict the spatiotemporal variability of soil salinity in the study area.' After having read the article, I think that this statement is not sufficiently supported by the results that were presented and discussed. You indeed evaluated whether time lapse EMI measurements can explain the total variation in a dataset of measured ECe values at different locations and depths and at different times. But, the question whether EMI can be used to monitor changes in ECe over time was not addressed and to my opinion it should be. You should evaluate whether the changes in ECe that are observed over time correspond with changes in EMI estimated ECe over time. When the answer to this question is negative, this paper shows that the spatial variations in ECe in the studied area are much larger than the temporal variations so that EMI can still be used to map spatial variations but not the temporal variability due to irrigation and seasonal leaching. Evaluating the temporal variability of ECe within a year might require to have also information about variation of soil water content, groundwater table depth and soil temperature, which also vary over time and modulate the variations of ECe over time.

Please see our detailed answer to the previous question and corresponding revision in this regard.

Ln 27: 'revealed salinity fluctuations related to the input of salts and water either through irrigation, precipitation or groundwater level and salinity.' You best reformulate this sentence. 'Salinity fluctuation related to salinity' is a circular explanation.

It refers to the salinity of groundwater. We revised the sentence to clarify this issue:

Old version (line 28)

"(...) through irrigation, precipitation or groundwater level and salinity."

New version

"(...) through irrigation, precipitation or level and salinity of groundwater."

Ln 100: How was reference ET obtained?

ET is calculated by the Penman-Monteith method and is given by information collected in the meteorological station shown in Figure 1.

Ln 119: Can you give some details about the soil samples? Soil rings or bulk samples? Which volume, mass of soil?

Bulk density (g m^{-3}) was determined once for each soil layer from undisturbed soil samples (100 cm^3) oven-dried at 105ºC. EC_e was measured in the extract collected with suction filters from disturbed soil samples, according to the method described by Richards (1954).

[Richards, L.A. (Ed.), 1954. Diagnosis and Improvement of Saline and Alkali Soils. Agricultural Handbook, USDA]

Old version (line 122)

"(...) after bulk density determination."

New version

"(...) after bulk density (g m^{-3}) determination from undisturbed 100 cm^3soil samples."

Old version (line 122)

"EC_e was measured with a conductivity meter (WTW 1C20-0211 inoLab) in the extract collected from the soil saturation paste."

New version

"EC_e was measured with a conductivity meter (WTW 1C20-0211 inoLab) in the extract collected from the soil saturation paste obtained from 300 g of air-dry soil samples, according to the methods described by Richards (1954)."

Old version (line 321)

" (...) 2397.2019019, 2019b.

Shanahan, P.W. (...)"

New version

" (...) 2397.2019019, 2019b.

Richards, L.A. (Ed.), 1954. Diagnosis and Improvement of Saline and Alkali Soils. Agricultural Handbook, USDA.

Shanahan, P.W. (...)"

Ln 139: 'The RMSE is the square root of the mean of the squared differences between the measured and predicted ECe, indicating how concentrated the data is around the linear regression' I am confused here. Which linear regression line are you referring to here? The linear regression between sigma and ECe that is based on the regional dataset and that you use to obtain ECe estimates from EMI measurements, which I would call ECep? Or the linear regression between ECep and the measured ECe from the soil samples? In case of the latter, you are 'correcting' the regional regression equation. At ln 140, you write: 'Lin's CCC measures the agreement between the measured and predicted ECe evaluating how close the linear regression is to the 1:1 relationship' This makes me wonder which regression equation you are talking about here. The regression between ECep and ECe measured? If that is the case, then the RMSE that you mention in ln 139 is not the mean of the squared differences between the measured and predicted ECe but it is the mean of the squared differences between the measured and the ECe's which are predicted using two sequential regressions: first you predict ECe form sigma to obtain ECep and then you make a linear regression between ECep and ECe measured and calculate the RMSE of the deviations between this regression and the measured ECe's. In order to avoid all these confusions, you should write the equations that you used to calculate the RMSE and the R^2 and you need to define clearly what are the 'predicted' ECe's: the ones obtained using the linear regression based on the regional calibration between sigma and ECe or the predictions by the regression between these predicted ECe's and the measured ECe's?

Please see our detailed answer to the previous question and corresponding revision in this regard.

Ln 154: for clarity, give the depths of ‘lower subsoil’, ‘intermediate subsoil’.

This information was already given in section 2.3 (lines 119 and 120) and also in the legend of Figure 3 (lines 165 and 166).

Ln 165: Figure 3: use the same horizontal axis for the different figures.

Corrected. Thank you.

Old version (Figure 3)

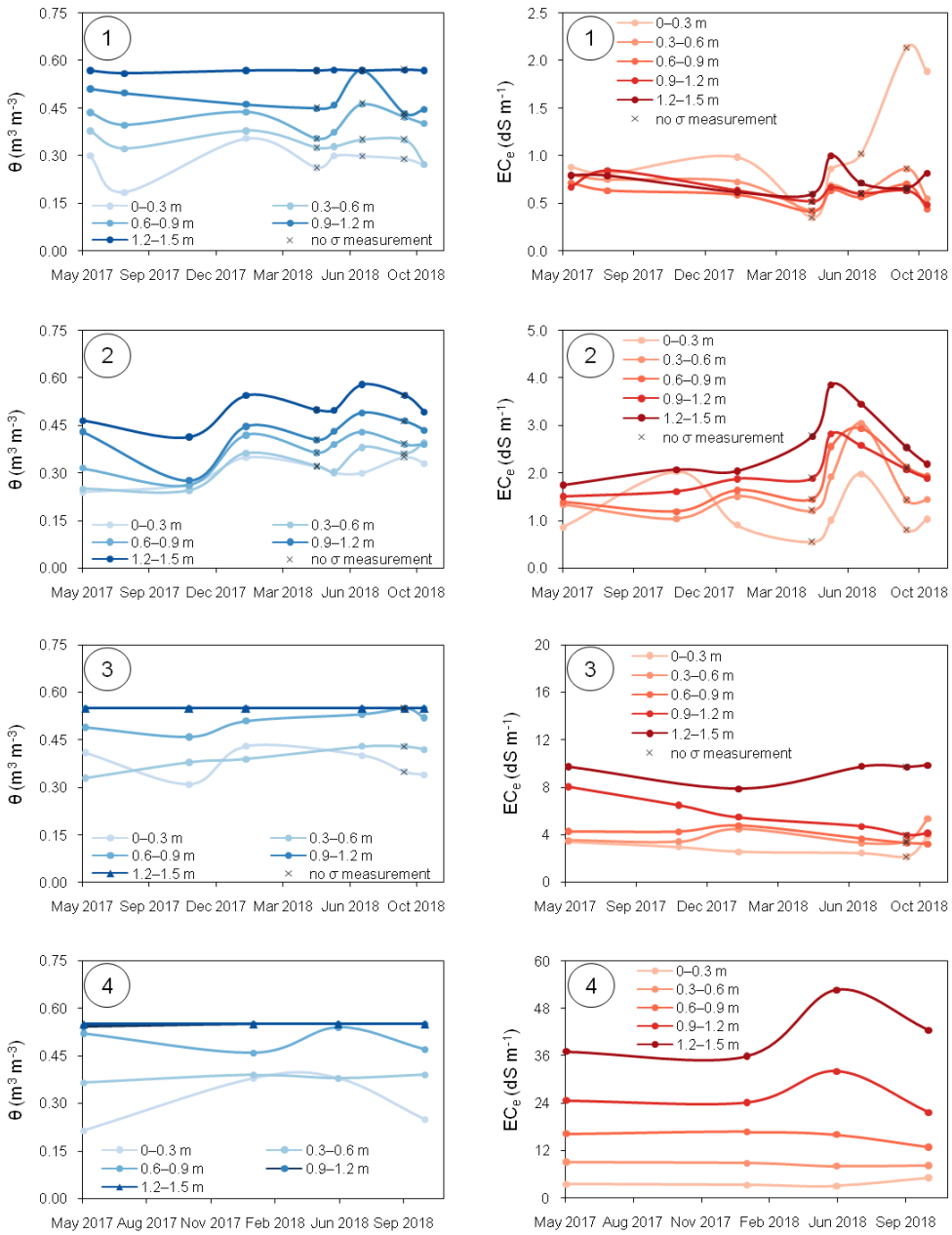

New version (Figure 3)

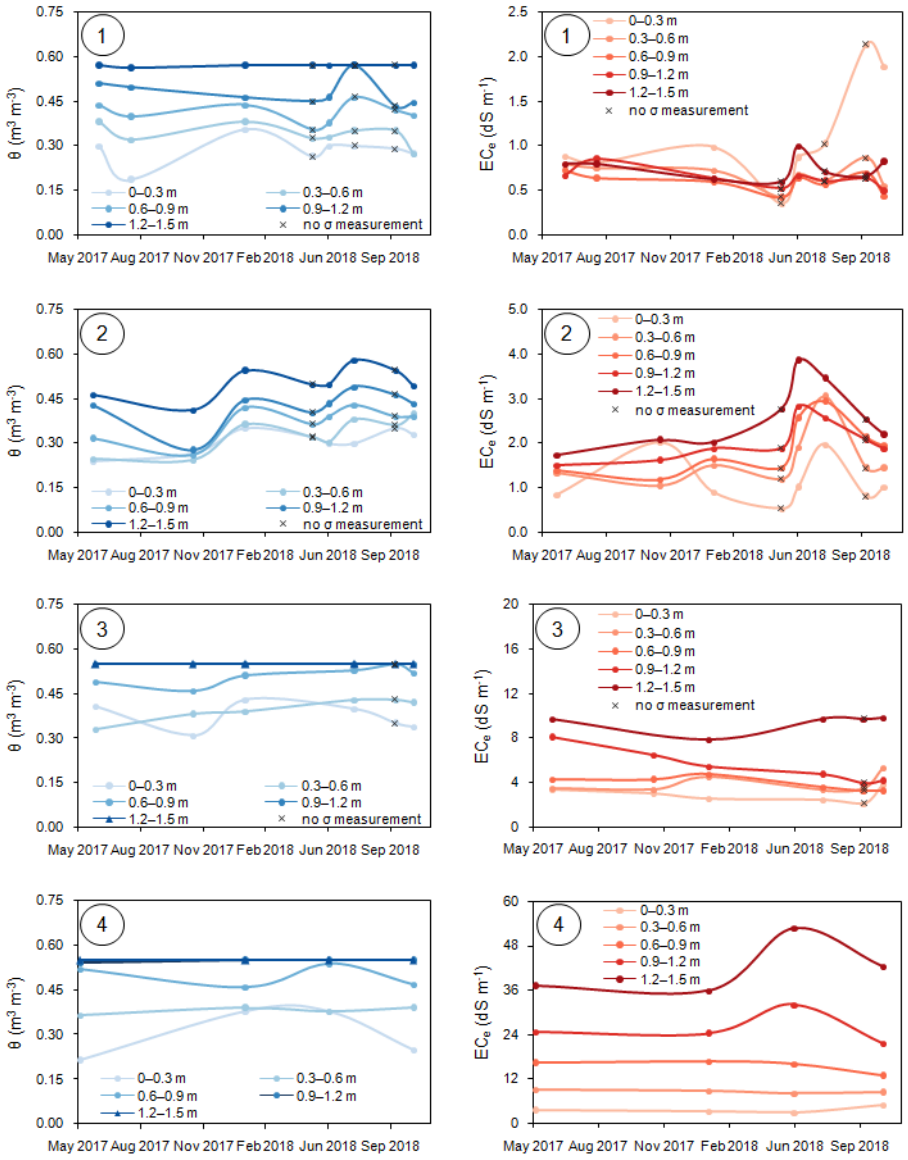

Ln 222: 'At location 4 the trend of increasing salinity with depth is accurate in all dates, but it tends to be slightly underestimated. The salinity maps show that salinity increases from non-saline in topsoil to severely-saline in lower subsoil.' How can I see in figure 5 that the trend is underestimated? I do not see that.

We mean that, at location 4, the predicted EC_e (which constitutes the maps) increases with depth, just like the measured EC_e at the sampling sites. However the predicted EC_e (in the background) is lower than the measured EC_e, which shows that predicted EC_e is underestimated.

Assessing soil salinity dynamics using time-lapse electromagnetic conductivity imaging~~Monitoring soil salinity using time-lapse electromagnetic conductivity imaging~~

Maria Catarina Paz [1,2], Mohammad Farzamian [1,3], Ana Marta Paz [3], Nádia Luísa Castanheira [3], Maria Conceição Gonçalves [3], Fernando Monteiro Santos [1]

[1]Instituto Dom Luiz, Faculdade de Ciências da Universidade de Lisboa, Campo Grande, Edifício C1, Piso 1, 1749-016 Lisboa, Portugal
[2]CIQuiBio, Barreiro School of Technology, Polytechnic Institute of Setúbal, Rua Américo da Silva Marinho, 2839-001 Lavradio, Portugal
[3]Instituto Nacional de Investigação Agrária e Veterinária, Avenida da República, Quinta do Marquês (edifício sede), 2780-157 Oeiras, Portugal

Correspondence to: Mohammad Farzamian (mohammad.farzamian@iniav.pt)

Abstract

Lezíria Grande of Vila Franca de Xira, located in Portugal, is an important agricultural system where soil faces the risk of salinization due to climate change, as the level and salinity of groundwater are likely to increase, as a result of the rise of the sea water level and consequently of the estuary. These changes can also affect the salinity of the irrigation water which is collected upstream of the estuary.~~Lezíria Grande of Vila Franca de Xira, located in Portugal, is an important agricultural system where soil faces the risk of salinization, being thus prone to desertification and land abandonment.~~ Soil salinity can be assessed over large areas by the following rationale: (1) use of electromagnetic induction (EMI) to measure the soil apparent electrical conductivity (EC_a, ~~dS~~ mS m^{-1}); (2) inversion of EC_a to obtain electromagnetic conductivity images (EMCI) which provide the spatial distribution of the soil electrical conductivity (σ, mS m^{-1}); (3) calibration process consisting of a regression between σ and the electrical conductivity of the saturated soil paste extract (EC_e, dS m^{-1}), used as a proxy for soil salinity; and (4) conversion of EMCI into salinity cross sections~~maps~~ using the obtained calibration equation. In this study, EMI surveys and soil sampling were carried out between May 2017 and October 2018 at four locations with different salinity levels across the study area of Lezíria de Vila Franca. A previously developed regional calibration was used for predicting EC_e from EMCI. Using time-lapse EMCI data, this study aims (1) to evaluate the ability of the regional calibration to predict soil salinity, and (2) to perform a preliminary qualitative analysis of soil salinity dynamics in the study area. The validation analysis showed that EC_e was predicted with a root mean square error (RMSE) of 3.14 dS m^{-1} in a range of 52.35 dS m^{-1}, slightly overestimated (−1.23 dS m^{-1}), with a strong Lin's concordance correlation coefficient (CCC) of 0.94 and high linearity between measured and predicted data (R^2 = 0.90). It was also observed that the prediction ability of the regional calibration is more influenced by spatial variability of data than temporal variability of data. Soil salinity cross sections were generated for each date and location of data collection, revealing qualitative salinity fluctuations related to the input of salts and water either through irrigation, precipitation, and level and salinity of groundwater. Time-lapse EMCI is developing into a valid methodology for evaluating the risk of soil salinization, so it can further support the evaluation and adoption of proper agricultural management strategies, especially in irrigated areas, where continuous monitoring of soil salinity dynamics is required.~~This study aims to evaluate the potential of time-lapse EMCI and the regional calibration to predict the spatiotemporal variability of soil salinity in the study area. The results showed that EC_e was satisfactorily~~

~~predicted, with a root mean square error (RMSE) of 3.22 dS m^{-1} in a range of 52.35 dS m^{-1} and a coefficient of determination (R^2) of 0.89. Results also showed strong concordance with a Lin's concordance correlation coefficient (CCC) of 0.93, although, EC_e was slightly overestimated with a mean error (ME) of −1.30 dS m^{-1}. Soil salinity maps for each location revealed salinity fluctuations related to the input of salts and water either through irrigation, precipitation or groundwater level and salinity.~~

~~Time lapse EMCI has proven to be a valid methodology for evaluating the risk of soil salinization, and can further support the evaluation and adoption of proper agricultural management strategies, especially in irrigated areas, where continuous monitoring of soil salinity dynamicsis required.~~

1 Introduction

Lezíria Grande de Vila Franca de Xira (hereafter called Lezíria de Vila Franca) is an important agricultural system of alluvial origin located by the estuary of river Tejo, northeast of Lisbon, Portugal (Fig. 1), where soil faces risk of salinization due to the marine origin of part of the sediments, tidal influence of the estuary, irrigation practices, and projected evolution of future climate with increasing temperature and decreasing precipitation. Traditional soil salinity investigations have been conducted in the study area using the electrical conductivity of a saturated soil paste extract (EC_e, dS m^{-1}) as a proxy for soil salinity. However, they were limited to few boreholes and involved soil sampling, which restricted the analysis to point information, often lacking representativeness at the field scale. In addition, borehole drilling is invasive and not feasible to conduct over large areas, given the large number of boreholes that needs to be made.

Electromagnetic induction (EMI) is widely used as a non-invasive and cost-effective solution to map soil properties over large areas. EMI measures the apparent electrical conductivity of the soil (EC_a, ~~dS~~ mS m^{-1}), which is a function of soil properties such as salinity, texture, cation exchange capacity, water content and temperature. However, in a saline soil, soil salinity is generally the dominant factor responsible for the spatiotemporal variability of soil EC_a when soil is moist.~~which is primarily a function of soil salinity, soil texture, water content, and cation exchange capacity; however, in a saline soil, soil salinity is generally the dominant factor responsible for the spatiotemporal variability of soil EC_a~~ EMI surveys have been successfully used in conjunction with soil sampling to assess soil salinity through location-specific calibration between measured EC_a and soil salinity (e.g. Triantafilis et al., 2000; 2001; Corwin and Lesch, 2005; Bouksila et al., 2012; Corwin and Scudiero, 2019; Kaufmann et al. 2019; von Hebel et al. 2019). However, the ability of this method for mapping soil salinity distribution with depth is limited. This is because EMI measures EC_a, a depth-weighted average conductivity measurement, which does not represent the soil electrical conductivity (σ, mS m^{-1}) with depth. More recently, a state-of-the-art approach called electromagnetic conductivity imaging (EMCI) has permitted to obtain σ from the inversion of multi-height and/or multi sensor EC_a data (Monteiro Santos, 2004; Dafflon et al., 2013; von Hebel et al., 2014; Farzamian et al., 2015; Shanahan et al., 2015; Jadoon et al, 2015; Moghadas et al., 2017). When comparing σ with the soil properties sampled in boreholes, such as EC_e, soil water content, pH, among others, a calibration process is developed through a regression between σ and the soil properties. This way, EMCI can be converted to a cross section~~map~~ of the soil properties which show

strong correlation with σ. This methodology has been applied in Lezíria de Vila Franca to study soil salinity risk (Farzamian et al., 2019; Paz et al., 2019b), and salinity and sodicity risk (Paz et al., 2019a) in which EMCI has been converted to EC_e and sodium adsorption ratio. In this later study, the authors performed a principal component analysis of the soil properties in the study area, and found that the water content was correlated with sigma, but with a relatively lower influence when compared to the properties related to salinity (EC_e, SAR and ESP).

Because the inversion of EC_a is relatively recent since the use of EMI for soil characterization, the lack of validation using an independent data set still limits the use of this new methodology (Corwin and Scudiero, 2019), making it therefore important to further test its accuracy in salinity monitoring.

When repeated over a period of time at the same place, EMCI becomes time-lapse EMCI and can be used to investigate the dynamics of soil properties such as soil water content (Huang et al., 2017; 2018; Moghadas et al., 2017). Using time-lapse EMCI data, this study aims (1) to evaluate the ability of a previously developed regional calibration to predict soil salinity, and (2) to perform a preliminary qualitative analysis of soil salinity dynamics in the study area. For this purpose, EMI measurements and soil sampling were carried out between May 2017 and October 2018 at four locations with different salinity levels across the study area. EMI measurements were performed with a single-coil instrument (EM38), collecting EC_a data in the horizontal and vertical orientations and at two heights, and then inverted to obtain EMCI, which provides a vertical distribution of σ. Finally, σ was converted to EC_e using the previously developed regional calibration. Soil samples were collected along the EMI transects, and used for laboratory determination of EC_e. These data were used as an independent dataset to evaluate the ability of the regional calibration to predict soil salinity, and to generate soil salinity cross sections for each date of data collection.~~When repeated over a period of time, EMCI of a study area is called time-lapse EMCI, and can be used to monitor the dynamics of soil salinity and other soil properties. Time-lapse EMCI has been successfully used to monitor soil water content (Huang et al., 2017; 2018; Moghadas et al., 2017) although, to our knowledge, its potential for monitoring soil salinity has not been previously investigated.~~

~~This study aims to evaluate the potential of time-lapse EMCI and a previously developed regional calibration to predict the spatiotemporal variability of soil salinity, and to monitor and evaluate soil salinity dynamics in the study area. For this purpose, EMI measurements and soil sampling were carried out between May 2017 and October 2018 at four locations with~~

~~different salinity levels across the study area. EMI measurements were performed with a single-coil instrument (EM38), collecting EC_a data in the horizontal and vertical orientations and at two heights, and then inverted to obtain EMCI, which provides a vertical distribution of σ. Finally, σ was converted to EC_e through the previously developed regional calibration. Soil samples were collected along the EMI transects, and used for laboratory determination of EC_e. These data were used as an independent test set to evaluate the ability of the regional calibration to predict the spatiotemporal variability of soil salinity, and to generate soil salinity maps for each date of data collection.~~

2 Material and methods

2.1 Study area

The study was carried out in Lezíria de Vila Franca, a peninsula of alluvial origin surrounded by the rivers Tejo and Sorraia, and the Tejo estuary, located 10 km northeast of Lisbon, Portugal, as shown in Fig. 1. Soils in this region have fine to very fine texture and are classified as Fluvisols in the northern part and as Solonchaks in the southern part, according to the Harmonized World Soil Database (Fischer et al., 2012). Climate is temperate with hot and dry summers, according to the Köppen classification. Daily measurements of precipitation, mean temperature and reference evapotranspiration recorded during the study period at the meteorological station represented by the blue circle in Fig. 1b, are shown in Fig. 2. Land use in this area (of about 130 km^2) is constituted by irrigated annual crops in the northern part and mainly by rainfed pastures in the southern part. Irrigation is assured by an infrastructure that covers most of the area, collecting surface water at the confluence of the two rivers. The irrigation water has low salinity with electrical conductivity typically below 0.5 dS m^{-1} and sodium adsorption ratio below 1 $(mmol_c\ L^{-1})^{0.5}$. The area exhibits a north-south soil salinity gradient which influences the distribution of land use types and which is probably due to the regional distribution of the marine fraction of sediments and to the saline influence of the estuary on groundwater in the southern part.

Four locations were chosen in the study area, as presented in Fig. 1b, with numbers 1 to 4. Locations 1, 2, and 3 are cultivated with annual rotations of irrigated herbaceous crops in spring and annual ryegrass (*Lolium multiflorum*) in the autumn, with ploughing usually once a year. During the study years (2017 and 2018), the spring crop at location 1 was tomato drip irrigated, and at locations 2 and 3 was maize irrigated by centre pivots. Location 4 is a rainfed spontaneous

pasture that hasn't been ploughed at least in the last ten years. During the study period, location 1 was irrigated from 12 April to 23 July 2017 and from 30 May to 23 September 2018; location 2 was irrigated from 17 June to 11 October 2017 and from 24 May to 22 September 2018; and location 3 was irrigated from 17 May to 10 September 2017 and from 06 June to 17 September 2018. Groundwater level is shallow, as expected in an estuarine environment, and has saline characteristics. In the southern part of the study area, closer to the estuary, the depth and salinity of groundwater are influenced by tidal variation.

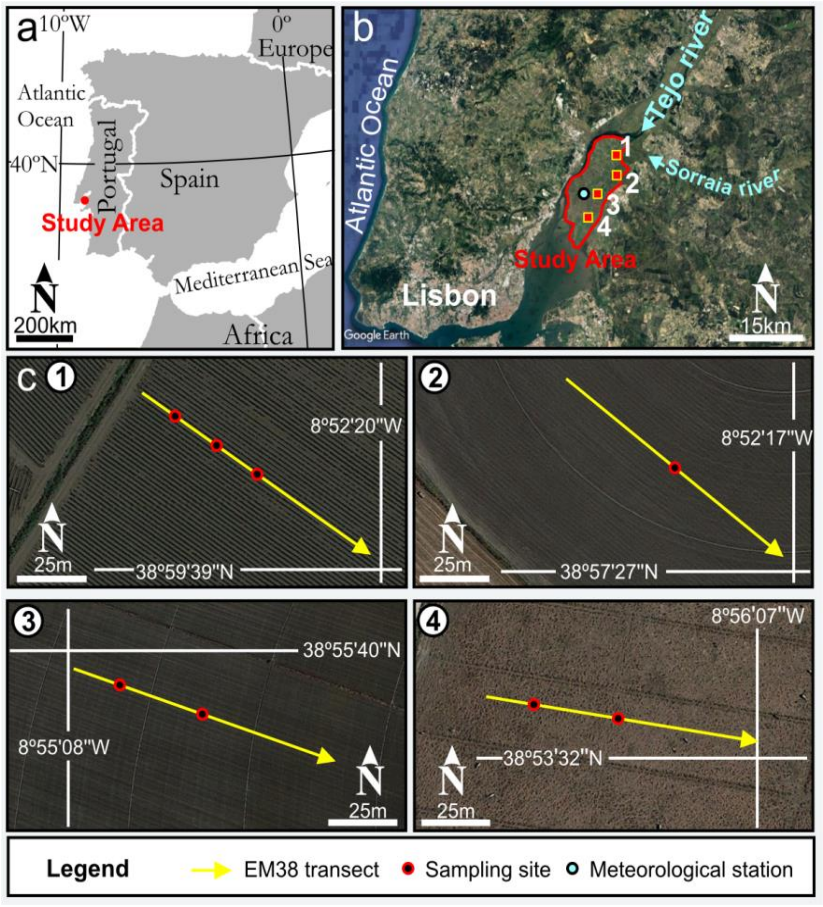

Figure 1: (a–b) Location of the study area in Portugal, showing the main geographical features and the four locations; (c) details of the four locations showing the EM38 transects and the soil sampling sites © Google Earth.

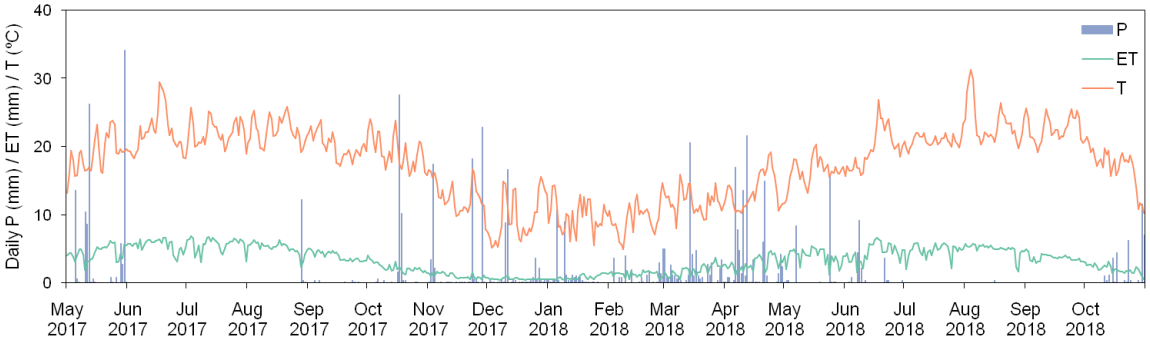

Figure 2: Distribution of daily precipitation (P), reference evapotranspiration (ET) and mean temperature (T) recorded at the meteorological station located in the study area during the study period.

2.2 Electromagnetic induction data acquisition and inversion

EMI data was acquired using the EM38 instrument (Geonics Ltd, Mississauga, Canada). Technology of this instrument is based on two coils, one transmitting the electromagnetic signal, and the other receiving it, distanced 1 m apart from each other inside the instrument case. The position of these coils can be controlled by placing the instrument in a vertical position relative to the soil surface - horizontal dipole mode (the coils stand in the horizontal position), which provides a maximum depth of investigation of 1.5 m - or in a horizontal position relative to the soil surface - vertical dipole mode (the coils stand in the vertical position), which provides a maximum depth of investigation of 0.75 m. EM38 surveys were done on five dates at locations 1 and 4, and on six dates at locations 2 and 3, during the period of May 2017 to October 2018. Measurements on the two first dates were continuously acquired at each location, along a 100 m transect, using a GPS (Rikaline 6010, with 5 m position accuracy) for registration of the position.~~Measurements on the two first dates were continuously acquired along 100 m transects using a GPS (Rikaline 6010) for registration of the position.~~ Subsequent EMI measurements were acquired at each location, along a 20 m transect. The middle point of each 20 m transect was coincident with the medium point of each previous 100 m transect. Measurements were acquired at positions 1 m apart along the 20 m transects (Fig. 1c), overlapping the medium section of the 100 m transects.~~positions 1 m apart along 20 m transects (Fig. 1c), overlapping the medium section of the 100 m transects.~~ EC_a was collected at two heights from the soil surface (0.15 and 0.4 m) in the horizontal and vertical dipole orientations, which was assured by placing the EM38 on a cart built specifically for this purpose. The cart has two shelves to accommodate the instrument, one at 0.15 m from the soil surface, and the other at 0.40 m from the soil surface. Inversion of EC_a data to obtain σ was carried out using a 1-D laterally constrained inversion

algorithm (Monteiro Santos et al., 2011). The EC_a responses of the model were calculated through forward modelling based on the full solution of the Maxwell equations (Kaufman and Keller, 1983). The subsurface model used in the inversion process consisted of a set of 1-D models distributed according to the position of the EC_a measurements. The subsurface model at each measurement position was constrained by the neighbouring models, allowing the use of the algorithm in regions characterized by high conductivity contrast. An Occam regularization (De Groot-Hedlin and Constable, 1990) based approach was used to invert the EC_a data. All EC_a data, collected at the four locations, were inverted by applying a five-layer earth initial model with electrical conductivity of 100 mS m^{-1} and a fixed layer thickness of 0.30 m. To run the algorithm, several parameters were selected, ~~To run the algorithm, several parameters are selected,~~ such as the type of inversion algorithm, the number of iterations, and the smoothing factor (λ) that controls the roughness of the model. The optimal inversion parameters for the present conditions were obtained in previous studies for the study area (Farzamian et al., 2019).

2.3 Soil sampling and laboratory analysis

Soil samples were collected at the same time of EMI surveys along the transects, as shown in Fig. 1c. At each sampling site, five soil samples were collected at 0.3 m increments, from a depth of 0.15 m to ~~to a depth of~~ 1.35 m, as a representation of topsoil (0−0.3 m), subsurface (0.3−0.6 m), upper subsoil (0.6−0.9 m), intermediate subsoil (0.9−1.2 m), and lower subsoil (1.2−1.5 m), to monitor water content and EC_e. In the laboratory, water content was obtained using the gravimetric method, and then converted to volumetric water content (θ – m^3 m^{-3}) after bulk density (g m^{-3}) determination from undisturbed 100 cm^3soil samples.~~determination~~. EC_e was measured with a conductivity meter (WTW 1C20-0211 inoLab) in the extract collected from the soil saturation paste obtained from 300 g of air-dry soil samples, according to the methods described by Richards (1954). In this study, the soil is classified according to its EC_e level as non-saline (EC_e<2 dS m^{-1}), slightly-saline (2–4 dS m^{-1}), moderately-saline (4–8 dS m^{-1}), highly-saline (8–16 dS m^{-1}), and severely saline (>16 dS m^{-1}), according to the terminology proposed by Barrett-Lennard et al. (2008).

2.4 Prediction of EC_e from time-lapse EMCI

A regional calibration to predict EC_e from σ was previously developed for the study area resulting in the linear equation $EC_e = 0.03\sigma - 1.05$ (Farzamian et al., 2019). This calibration was termed “regional” because the equation was obtained using

all EC_e and σ data collected at four locations in the study area. Farzamian et al. (2019) tested the regional and location-specific calibrations, verifying that they have comparable prediction ability. However, the regional calibration can be used at any new location in the study area, within the range of measured EC_e, which makes it highly suitable for mapping salinity in the study area. ~~However, the regional calibration can be used at any new location in the study area, within the range of measured EC_e, which makes it highly suitable for mapping and monitoring salinity in the study area.~~ The regional calibration was based on data collected during May and June 2017 and was validated using a leave-one-out-cross-validation method with good results (RMSE = 2.54 dS m^{-1} in the 0–37 dS m^{-1} range). The detailed calibration and cross-validation procedures are described in Farzamian et al. (2019).

In the present study, the regional calibration was used to predict EC_e from time-lapse EMCI (pEC_e). The predicted EC_e and EC_e measured from soil samples (mEC_e), collected at the same time as the EMI surveys, were used as an independent data set for the validation of the regional calibration. The validation was performed by calculating the root mean square error (RMSE), the coefficient of determination (R^2) between the measured and predicted EC_e, the Lin's concordance correlation coefficient (CCC), and the mean error (ME). Description of these statistical indicators and the equations used to calculate them are shown in Table 1. Calculations were done using global data, and also using data discriminated by date of measurement (in this case we considered dates when measurements were done at the four locations – January, June and October 2018), depth of measurement and location. ~~In the present study, the regional calibration was used to predict EC_e from time-lapse EMCI. The predicted EC_e and EC_e measured from soil samples, collected from July 2017 to October 2018, were used to validate the regional calibration as an independent test set. Its prediction ability was evaluated by calculating the root mean square error (RMSE), the coefficient of determination (R^2) between the measured and predicted EC_e, the Lin's concordance correlation coefficient (CCC), and the mean error (ME). The RMSE is the square root of the mean of the squared differences between the measured and predicted EC_e, indicating how concentrated the data is around the linear regression. In this study we used two degrees of freedom for a more robust calculation of RMSE. The coefficient of determination (R^2) indicates how well the predicted EC_e approximate the measured EC_e. When this is 1, it means the predictions coincide with the measurements. Lin's CCC measures the agreement between the measured and predicted EC_e evaluating how close the linear regression is to the 1:1 relationship and ranges from −1 to 1, with perfect agreement at 1 (Lin,~~

~~1989). ME is the mean of all differences between the measured and predicted EC_e and evaluates whether the linear regression consistently over- and underestimates the predicted EC_e. Therefore, the prediction is more precise and less biased when the RMSE and the ME are closer to zero.~~

Table 1 – Description and equations of the statistical indicators used to evaluate the prediction ability of the regional calibration in this work.

Statistics	Equation[1]	Description
Root mean square error (RMSE)	$\mathrm{RMSE} = \sqrt{\frac{\sum_{i=1}^{n}(mEC_{e_i} - pEC_{e_i})^2}{n-2}}$	Evaluates matching between measured and predicted data. When it is zero, it indicates perfect matching between measured and predicted data.
Mean error (ME)	$\mathrm{ME} = \frac{\sum_{i=1}^{n}(mEC_{e_i} - pEC_{e_i})}{n}$	Evaluates whether the predicted data are over- or underestimated. A negative value means overestimation, a positive value means underestimation.
Lin's concordance correlation coefficient (Lin's CCC)	$\mathrm{Lin's\ CCC} = \frac{2s_{mEC_e - pEC_e}}{s_{mEC_e}^2 + s_{pEC_e}^2 + (\overline{mEC_{e_i}} - \overline{pEC_{e_i}})^2}$	Evaluates agreement between measured and predicted data. Ranges from -1 to 1. When it is 1, it indicates perfect agreement between measured and predicted data (Lin, 1989).
Coefficient of determination (R^2)	$R^2 = \left(\frac{\sum_{i=1}^{n}(mEC_{e_i} - \overline{mEC_{e_i}})(pEC_{e_i} - \overline{pEC_{e_i}})}{\sqrt{\sum_{i=1}^{n}(mEC_{e_i} - \overline{mEC_{e_i}})^2}\sqrt{\sum_{i=1}^{n}(pEC_{e_i} - \overline{pEC_{e_i}})^2}}\right)^2$	Indicates the degree of linearity between predicted and measured data. Ranges from 0 to 1. Above 0.5 is considered satisfactory.

[1]n is the total number of data; mEC_e is measured EC_e; pEC_e is predicted EC_e; the upper bar represents the mean of the indicated data.

4 Results and discussion

4.1 Temporal variation of measured θ and EC_e

Figure 3 shows the variation of θ and EC_e with time at the sampling site located in the middle of each transect (Fig. 1c), at locations 1 to 4. At location 1, θ increases with depth and the lower subsoil (1.2–1.5 m) is permanently saturated within the study period. In the more superficial layers until 0.9 m depth, the influence of rainfall, evapotranspiration, and irrigation is noticeable. For instance, in the topsoil, θ peaks in January 2018 and lowers during the dry seasons, because drip irrigation during the dry seasons has a localized effect and there is high water uptake by the crop. At location 2, unlike the other

locations, the lower subsoil is unsaturated. The influence of rainfall, evapotranspiration and irrigation is also noticeable. At locations 3 and 4, θ also increases with depth and the intermediate and lower subsoil layers are permanently saturated.

Regarding EC_e, at location 1 the values observed are always below 1 dS m^{-1}, except for the topsoil in September and October 2018, which is probably due to fertigation practises during the irrigation period. At location 2, EC_e generally increases with depth. All layers show a peak in June and July 2018, probably due to fertigation practises. At location 3, EC_e reaches higher levels than at the previous locations, exceeding 4 dS m^{-1}, which is the generally accepted threshold for the classification of saline soils. Location 4 presents the highest EC_e of all locations. At the topsoil the values are below 4 dS m^{-1}, but increase consistently with depth to about 50 dS m^{-1} in the lower subsoil. The increase of EC_e during June 2018 can be due to the influence of saline groundwater.

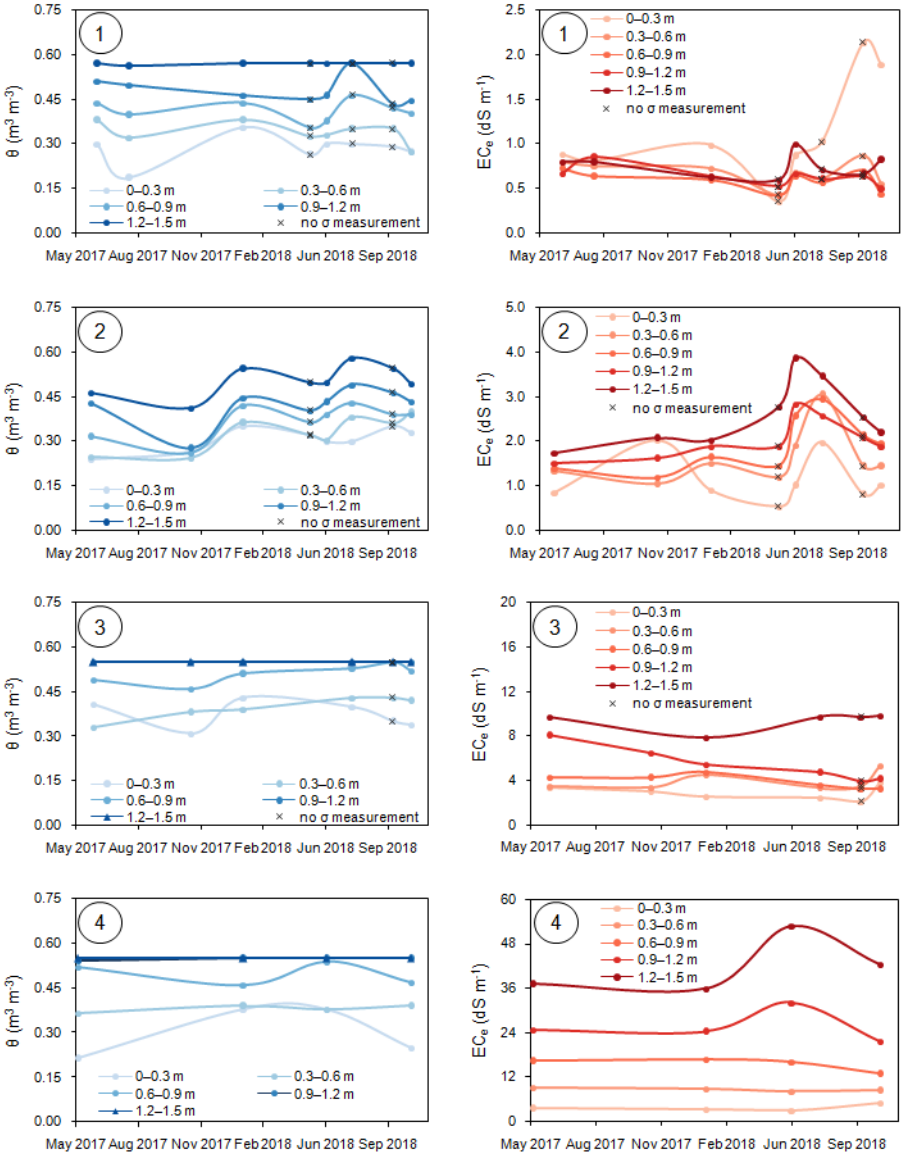
1
θ (m³ m⁻³)
0.75
0.60
0.45
0.30
0.15
0.00
0–0.3 m
0.3–0.6 m
0.6–0.9 m
0.9–1.2 m
1.2–1.5 m
no σ measurement
May 2017 Aug 2017 Nov 2017 Feb 2018 Jun 2018 Sep 2018
1
ECe (dS m⁻¹)
2.5
2.0
1.5
1.0
0.5
0.0
0–0.3 m
0.3–0.6 m
0.6–0.9 m
0.9–1.2 m
1.2–1.5 m
no σ measurement
May 2017 Aug 2017 Nov 2017 Feb 2018 Jun 2018 Sep 2018
2
θ (m³ m⁻³)
0.75
0.60
0.45
0.30
0.15
0.00
0–0.3 m
0.3–0.6 m
0.6–0.9 m
0.9–1.2 m
1.2–1.5 m
no σ measurement
May 2017 Aug 2017 Nov 2017 Feb 2018 Jun 2018 Sep 2018
2
ECe (dS m⁻¹)
5.0
4.0
3.0
2.0
1.0
0.0
0–0.3 m
0.3–0.6 m
0.6–0.9 m
0.9–1.2 m
1.2–1.5 m
no σ measurement
May 2017 Aug 2017 Nov 2017 Feb 2018 Jun 2018 Sep 2018
3
θ (m³ m⁻³)
0.75
0.60
0.45
0.30
0.15
0.00
0–0.3 m
0.3–0.6 m
0.6–0.9 m
0.9–1.2 m
1.2–1.5 m
no σ measurement
May 2017 Aug 2017 Nov 2017 Feb 2018 Jun 2018 Sep 2018
3
ECe (dS m⁻¹)
20
16
12
8
4
0
0–0.3 m
0.3–0.6 m
0.6–0.9 m
0.9–1.2 m
1.2–1.5 m
no σ measurement
May 2017 Aug 2017 Nov 2017 Feb 2018 Jun 2018 Sep 2018
4
θ (m³ m⁻³)
0.75
0.60
0.45
0.30
0.15
0.00
0–0.3 m
0.3–0.6 m
0.6–0.9 m
0.9–1.2 m
1.2–1.5 m
May 2017 Aug 2017 Nov 2017 Feb 2018 Jun 2018 Sep 2018
4
ECe (dS m⁻¹)
60
48
36
24
12
0
0–0.3 m
0.3–0.6 m
0.6–0.9 m
0.9–1.2 m
1.2–1.5 m
May 2017 Aug 2017 Nov 2017 Feb 2018 Jun 2018 Sep 2018

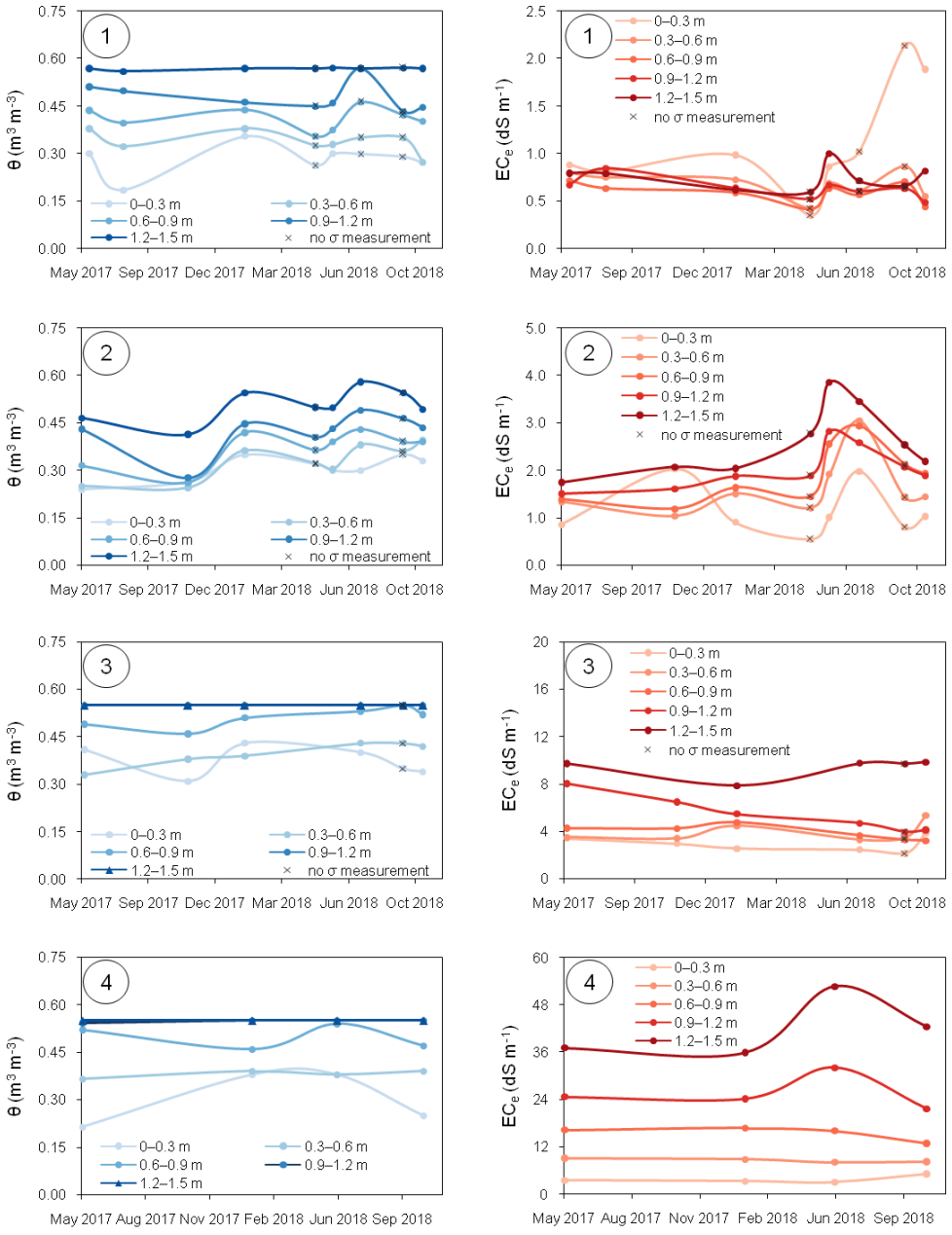

230 **Figure 3: Volumetric water content (θ – m^3 m^{-3}) and electrical conductivity of the soil saturation extract (EC_e – dS m^{-1}), in the topsoil (0–0.3 m), subsurface (0.3–0.6 m), upper subsoil (0.6–0.9 m), intermediate subsoil (0.9–1.2 m), and lower subsoil (1.2–1.5 m), measured** in the sampling site located at the middle of each transect, at locations 1 to 4, during the study period. Each circled number refers to each location. Crosses refer to the dates when there were ECe measurements but no σ measurements, due to adverse field conditions.~~at the sampling site located in the middle of each transect, at locations 1 to 4, during the study period.~~

235

4.2. Time-lapse EMCIs

Figure 4 shows the obtained EMCIs at locations 1 to 4 for each date of the EMI surveys. Globally, σ ranges from 19.44 mS m^{-1} to 1431.57 mS m^{-1} with the lowest values at location 1 and the highest at location 4. A general increasing trend of σ is quite evident from the north to the south, accompanying the previously known soil salinity gradient. In addition, σ increases with depth at locations 2, 3 and 4. At location 1, σ ranges spatiotemporally from 19.44 mS m^{-1} to 128.08 m^{-1}. At location 2, σ ranges from 28.02 mS m^{-1} to 469.39 mS m^{-1} with highest values at depth. A similar pattern of σ is evident at locations 3 and 4. However, a greater range of σ is seen at location 3 with values from 36.23 mS m^{-1} to 706.32 mS m^{-1}. Location 4 exhibits the largest variations of σ, ranging from 48.57 mS m^{-1} to 1431.57 mS m^{-1}.

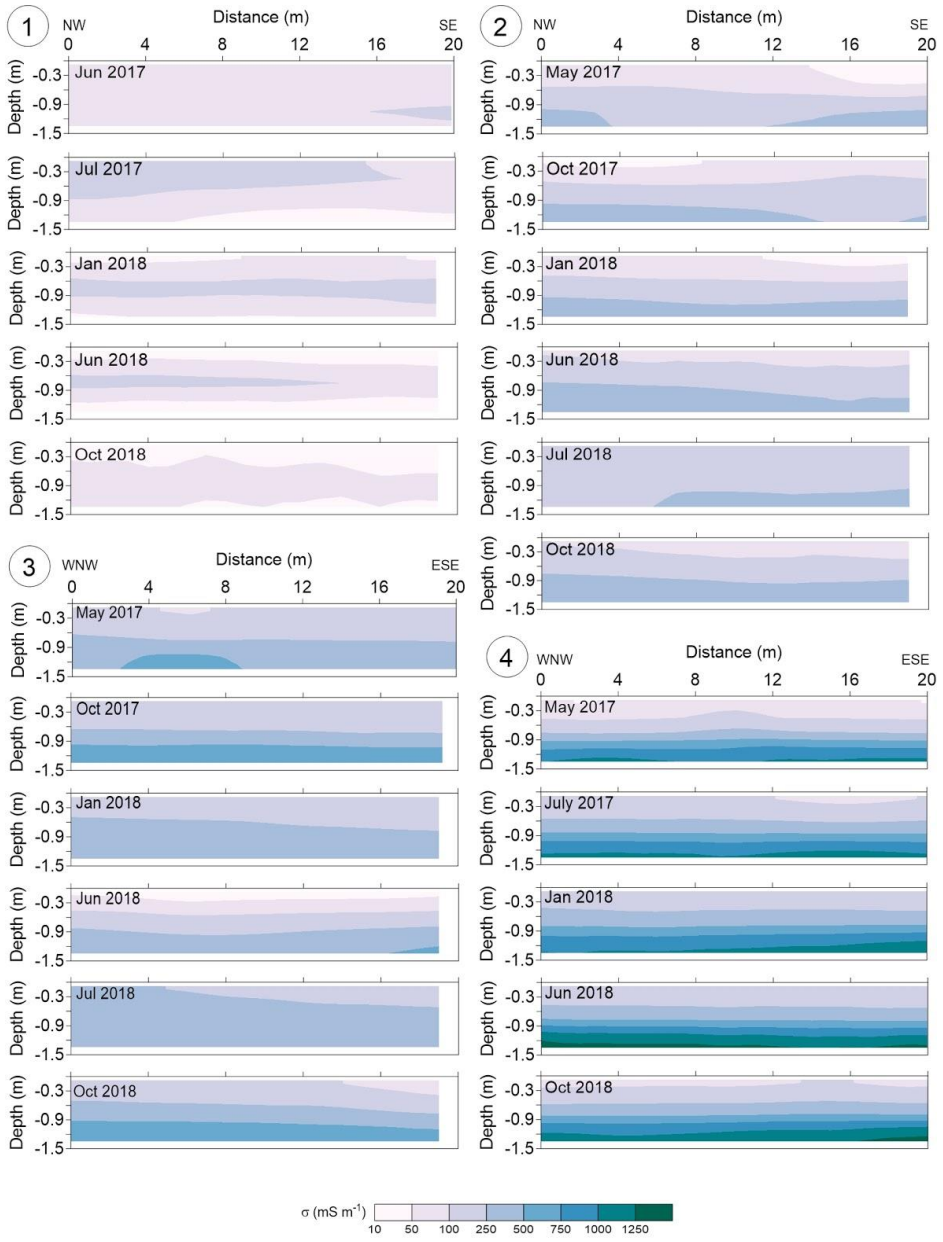

Figure 4: Time-lapse electromagnetic conductivity images (EMCIs) for locations 1 to 4.

4.~~2~~ 3 Prediction of EC_e using the regional calibration

For a specific evaluation of the prediction ability of the regional calibration, Table 2 shows the statistical indicators obtained using global data, i.e., data collected at all locations, from July 2017 to October 2018, and the statistical indicators for each date, soil depth, and location. The validation of the regional calibration using global data resulted in a RMSE of 3.14 dS m^{-1}

and R^2 of 0.90, which indicates satisfactory prediction ability, given the large range of EC_e (52.35 dS m^{-1}). The high global Lin's CCC of 0.94 shows agreement between measured and predicted EC_e. The ME is −1.23 dS m^{-1}, indicating that the regional calibration generally overestimates EC_e. The statistical indicators discriminated by date of measurement (in this case we considered only the dates when measurements were done at the four locations – January, June and October 2018), shown in Table 2, also indicate that the prediction ability doesn't vary significantly when comparing the statistical indicators of the three dates. The validation procedure used in this study gives slightly lower prediction ability for the regional calibration than the previously obtained with the leave-one-out-cross-validation (see section 2.4). This is expected as this dataset is completely independent from the dataset used to develop the calibration and was collected over a wider period of time (18 months). During this period, soil properties, which are also known to influence σ, such as temperature and θ, change, which introduces larger variability in data.

In terms of the influence of depth of measurement, prediction ability improves with depth, being weak at top soil, and very good from the subsurface to the lower subsoil. We attribute the weak prediction ability at top soil to the smaller range of EC_e variability (0.35–5.17 dS m^{-1}) and to the larger variability of other soil properties (e.g. θ and temperature), which are due to different irrigation schemes and cultivated crops at each location. In terms of the influence of each location, prediction ability varies considerably. At location 1, prediction ability is very poor, with a low R^2, which means the degree of linearity between predicted and measured data is low, and a high RMSE within the considered range of EC_e. At this location, however, the soil is non-saline and the range of EC_e, is very small (0.35–1.89 dS m^{-1}) and thus other soil properties such as θ and clay content have larger impact on spatiotemporal variability of σ. At locations 2, 3 and 4, prediction ability of the regional calibration is acceptable at the former two, and good at the latter. We can analyse better these results when observing Fig. 5, which shows EC_e predicted with the regional calibration versus the measured EC_e and the 1:1 line, with data identified in terms of date of measurement (Fig. 5a) and depth of measurement (Fig. 5b). Fig. 5c and Fig. 5d display an enlargement of the lower left part of the previous figures, displaying EC_e values below 15 dS m −1, and data relative to locations 1, 2 and 3 at different depths. At location 2, EC_e is more overestimated in deeper soil layers (Fig. 5d) which is likely due to the clay content that consistently increases with depth at this location, while it is rather uniform or declines with depth at the other locations (Farzamian et al., 2019). This is probably also the main reason for the very low Lin's CCC at this location. At location 3, EC_e is also overestimated (Fig. 5d), most likely due to the influence of θ and cation exchange capacity (Paz et al., 2019a) which are higher on average compared to locations 2 and 4. Finally, the EC_e ranges of location 4 and of the lower subsoil are similar to the EC_e range of global data, showing dominance of location 4 and of lower subsoil data on the calibration.

These results show that spatial variability of data has a much stronger influence on the prediction ability of the regional calibration, than temporal variability of data. This spatial sensitivity of the regional calibration can be improved by studying new locations across the study area to include a wider variability of soil properties and ranges of EC_e in the calibration process. On the other hand, longer observation periods and more frequent EMI surveying and soil sampling, as well as monitoring of other soil dynamic properties that influence σ (i.e. θ, soil temperature, level and salinity of groundwater) and

finding ways to quantitatively account for their impact on time-lapse EMCIs, can improve the temporal sensitivity of regional calibration.

Table 2 – RMSE, ME, Lin's CCC, R2, minimum, maximum and range of ECe, and the number of data used to calculate these statistical indicators, discriminated in terms of global, date of measurement, depth of measurement and location.

	RMSE (dS m^{-1})	ME (dS m^{-1})	Lin's CCC	R^2	EC_e min (dS m^{-1})	EC_e max (dS m^{-1})	EC_e range (dS m^{-1})	Number of data
Global	3.14	−1.23	0.94	0.90	0.35	52.70	52.35	103
Jan 2018	2.79	−1.33	0.96	0.93	0.59	35.90	35.31	30
Jun 2018	4.27	−0.08	0.94	0.94	0.35	52.70	52.35	20
Oct 2018	3.11	−0.71	0.96	0.93	0.44	42.50	42.06	19
0–0.3 m	1.79	−0.39	0.39	0.19	0.35	5.17	4.82	21
0.3–0.6 m	1.74	−0.34	0.78	0.67	0.42	8.86	8.44	21
0.6–0.9 m	2.40	−1.61	0.89	0.91	0.42	16.72	16.30	21
0.9–1.2 m	4.77	−3.25	0.89	0.89	0.49	32.10	31.61	21
1.2–1.5 m	4.71	−0.87	0.95	0.93	0.60	52.70	52.10	20
Location 1	1.23	−0.59	−0.05	0.02	0.35	1.89	1.54	35
Location 2	3.22	−2.40	0.23	0.56	0.91	3.86	2.95	24
Location 3	3.88	−2.56	0.44	0.47	1.98	9.85	7.87	24
Location 4	4.63	0.65	0.94	0.90	2.33	52.70	50.37	20

~~Figure 4 shows EC_e predicted with the regional calibration versus the measured EC_e and the 1:1 line, with points identified in terms of date of measurement (Fig. 4a) and depth of measurement (Fig. 4b). Prediction of EC_e with the regional calibration using data collected from July 2017 to October 2018 resulted in a RMSE of 3.22 dS m^{-1} and R^2 of 0.89, which indicates satisfactory prediction ability, given the large range of EC_e (52.35dS m^{-1}). The high global Lin's CCC of 0.93 shows accord between measured and predicted EC_e. The ME is −1.30 dS m−1, indicating that the regional calibration globally overestimates EC_e. Figure 4a and Fig. 4b show that the points are generally scattered around the 1:1 line and it is not possible to identify variations depending on the date or depth of the measurement. In order to analyze the prediction ability at each location, Fig. 4c and Fig. 4d display an enlargement of the lower left part of the previous figures, displaying EC_e values below 15 dS m^{-1}. Figure 4c and Fig. 4d show differences in the prediction ability according to the location, namely at locations 2 and 3, where EC_e is generally overestimated. At location 2, EC_e is more overestimated in deeper soil layers (Fig. 4d) which is likely due to a previously identified influence of clay content that consistently increases with depth at this location, while it is rather uniform or declines with depth at the other locations (Farzamian et al., 2019).~~

~~The validation procedure used in this study gives lower prediction ability for the regional calibration than the previously obtained with the leave one out cross validation (see section 2.4). This can be justified because the test set is completely independent from the dataset used to develop the calibration. Furthermore, this test set is composed of measurements collected over a wider period of time (18 months). During this period, soil properties, which are also known to influence σ, such as θ, change (as shown in Fig. 3), which introduces larger variability in the measurements. However, and given the large range of EC_e (52.35 dS m^{-1}), a RMSE of 3.22 dS m^{-1} is acceptable for this type of non-invasive and indirect method. The regional calibration could be further developed by including measurements taken over a longer period of time in the calibration process, in order to include a wider range of variation of soil properties.~~

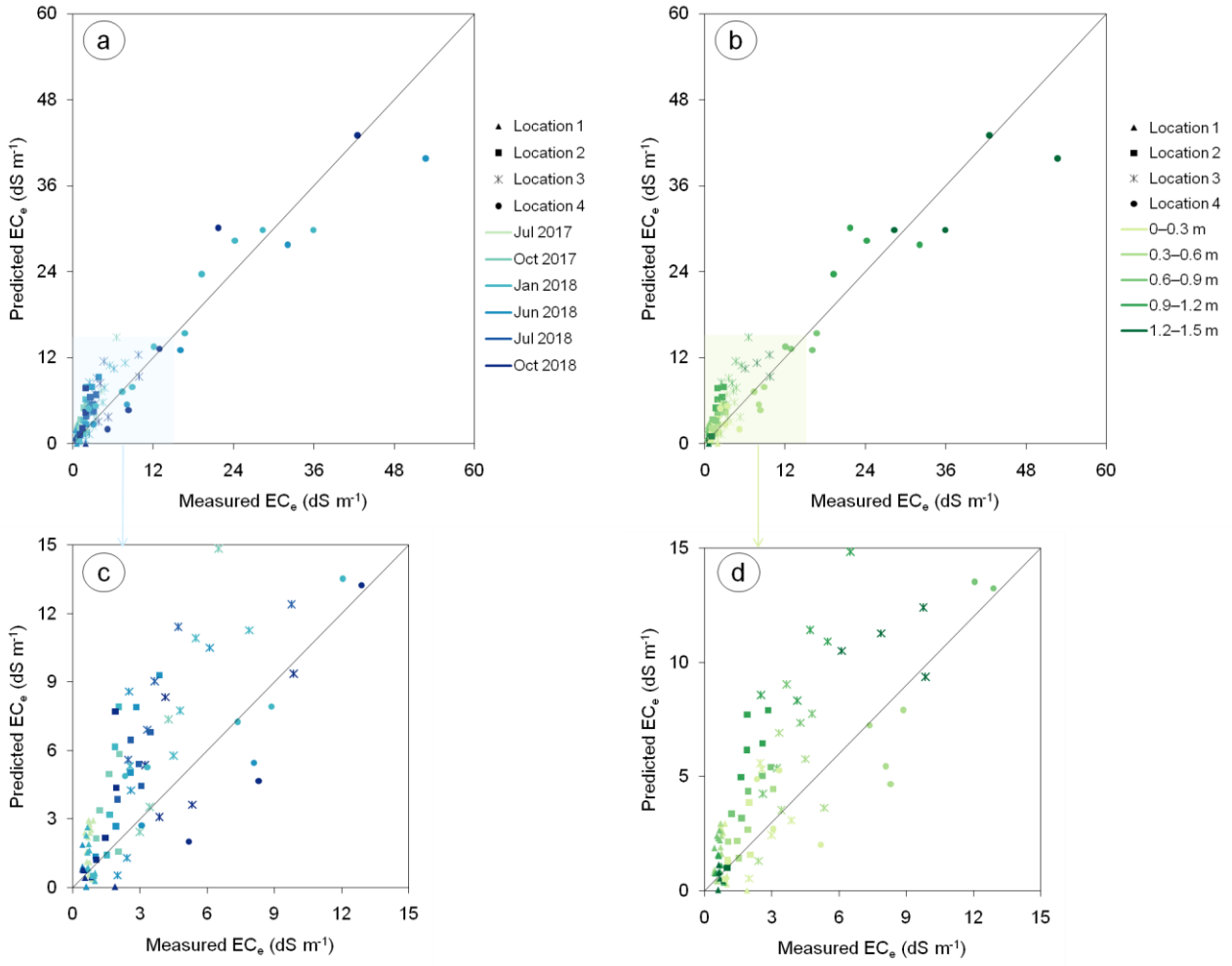
a
b
c
d
Predicted EC_e (dS m^{-1})
Measured EC_e (dS m^{-1})
Location 1
Location 2
Location 3
Location 4
Jul 2017
Oct 2017
Jan 2018
Jun 2018
Jul 2018
Oct 2018
0–0.3 m
0.3–0.6 m
0.6–0.9 m
0.9–1.2 m
1.2–1.5 m

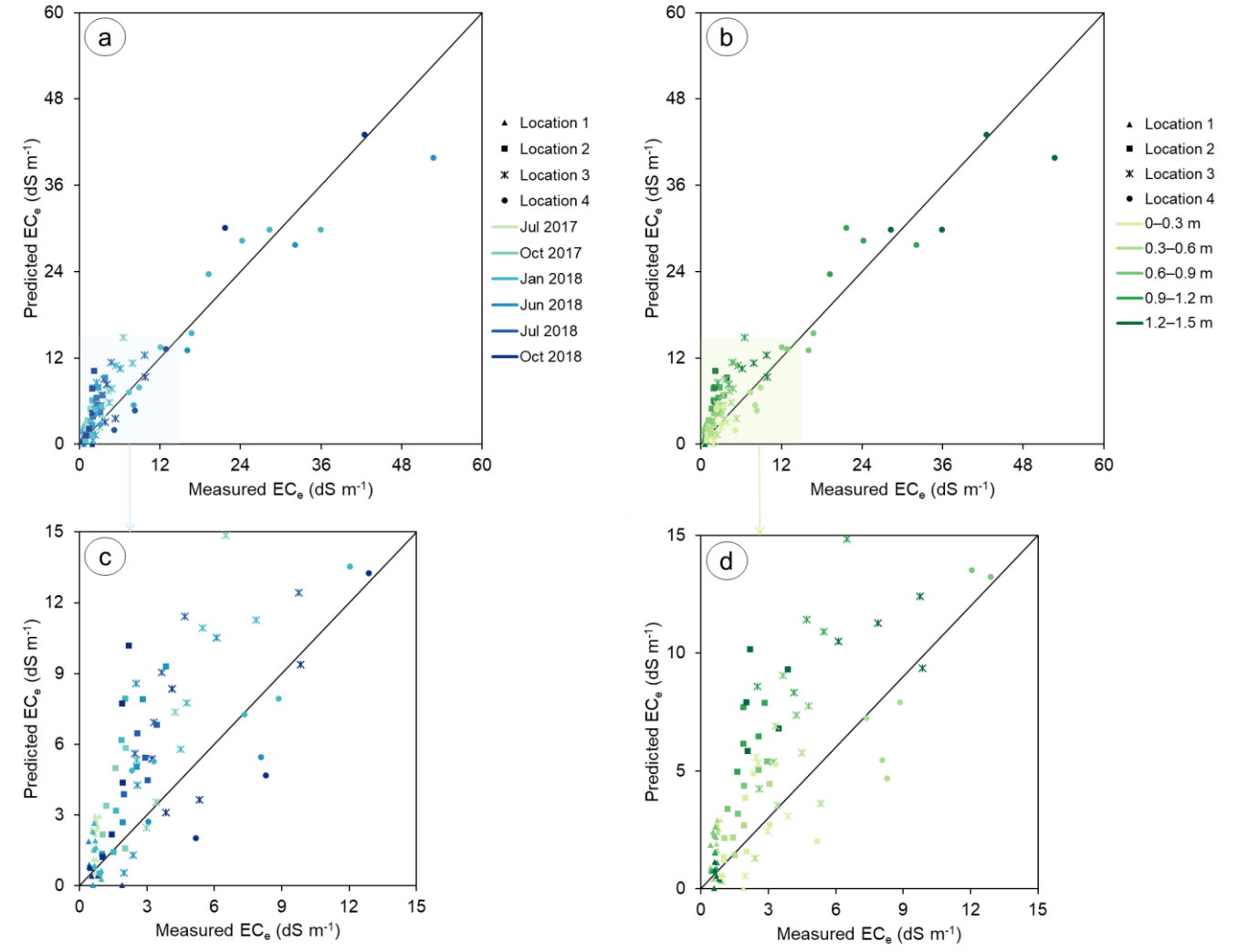

Figure ~~4~~ 5: Plots of predicted EC_e versus measured EC_e and the 1:1 line, obtained for locations 1 to 4, identified in terms of date of measurement (a) and depth of measurement (b). Plots (c) and (d) show enlargements of the lower left part of plots (a) and (b), respectively.

4.4 Generation of soil salinity cross sections from time-lapse EMCI~~4.3 Spatiotemporal mapping of soil salinity from time-lapse EMCI~~

Figure ~~5~~ 6 shows the soil salinity cross sections~~maps~~ (EC_e predicted using the regional calibration) at locations 1 to 4 for each date of the EMI surveys, categorized into 6 salinity classes, ranging from non-saline to severely-saline. The measured EC_e and the groundwater level at the sampling site located in the middle of each EMI transect are also shown.

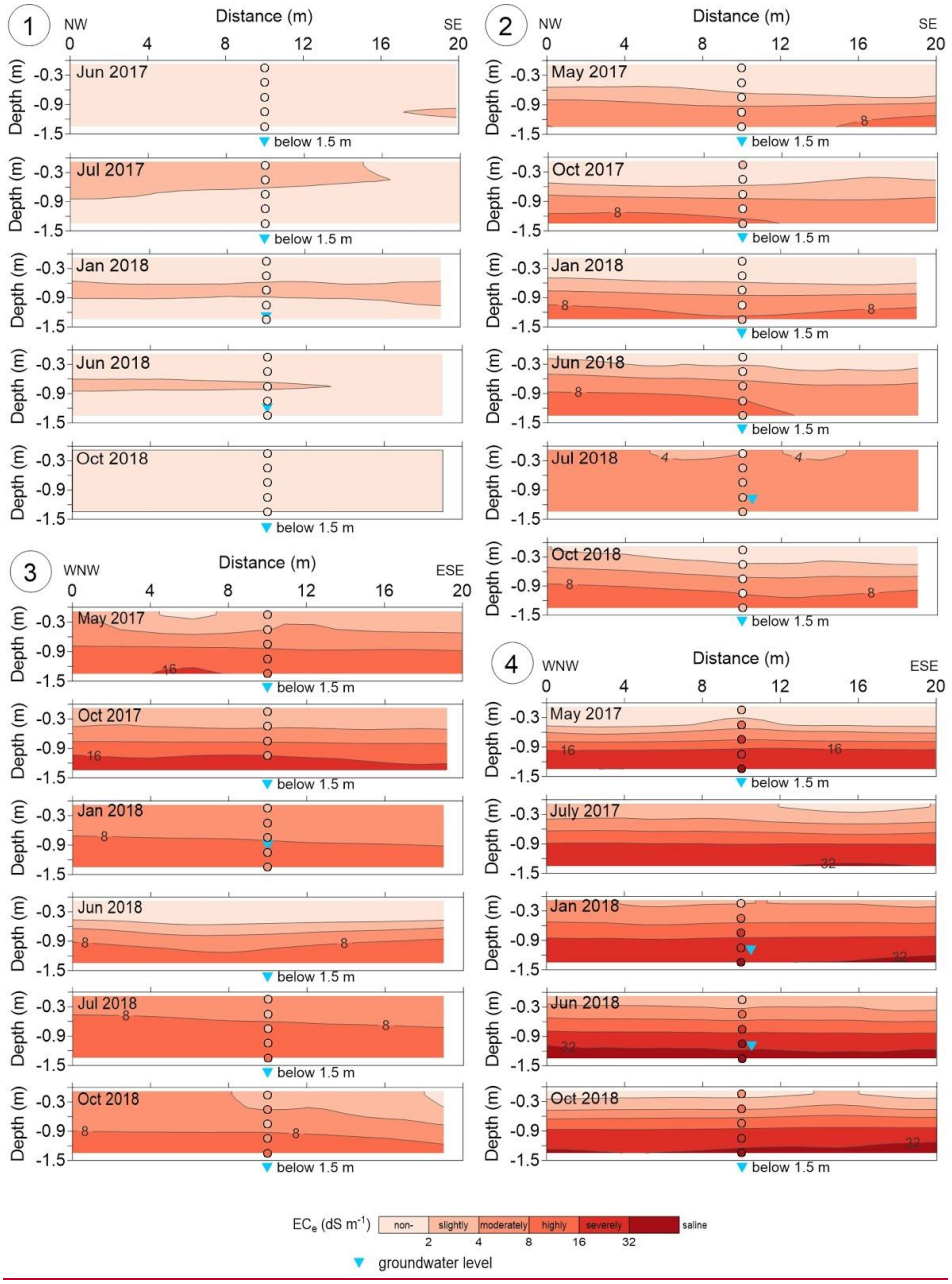
1
NW
Distance (m)
SE
0
4
8
12
16
20
Depth (m)
-0.3
-0.9
-1.5
Jun 2017
Jul 2017
Jan 2018
Jun 2018
Oct 2018
below 1.5 m
2
NW
Distance (m)
SE
May 2017
Oct 2017
Jan 2018
Jun 2018
Jul 2018
Oct 2018
below 1.5 m
3
WNW
Distance (m)
ESE
May 2017
Oct 2017
Jan 2018
Jun 2018
Jul 2018
Oct 2018
below 1.5 m
4
WNW
Distance (m)
ESE
May 2017
July 2017
Jan 2018
Jun 2018
Oct 2018
below 1.5 m
ECe (dS m-1)
non-
slightly
moderately
highly
severely
saline
2
4
8
16
32
groundwater level

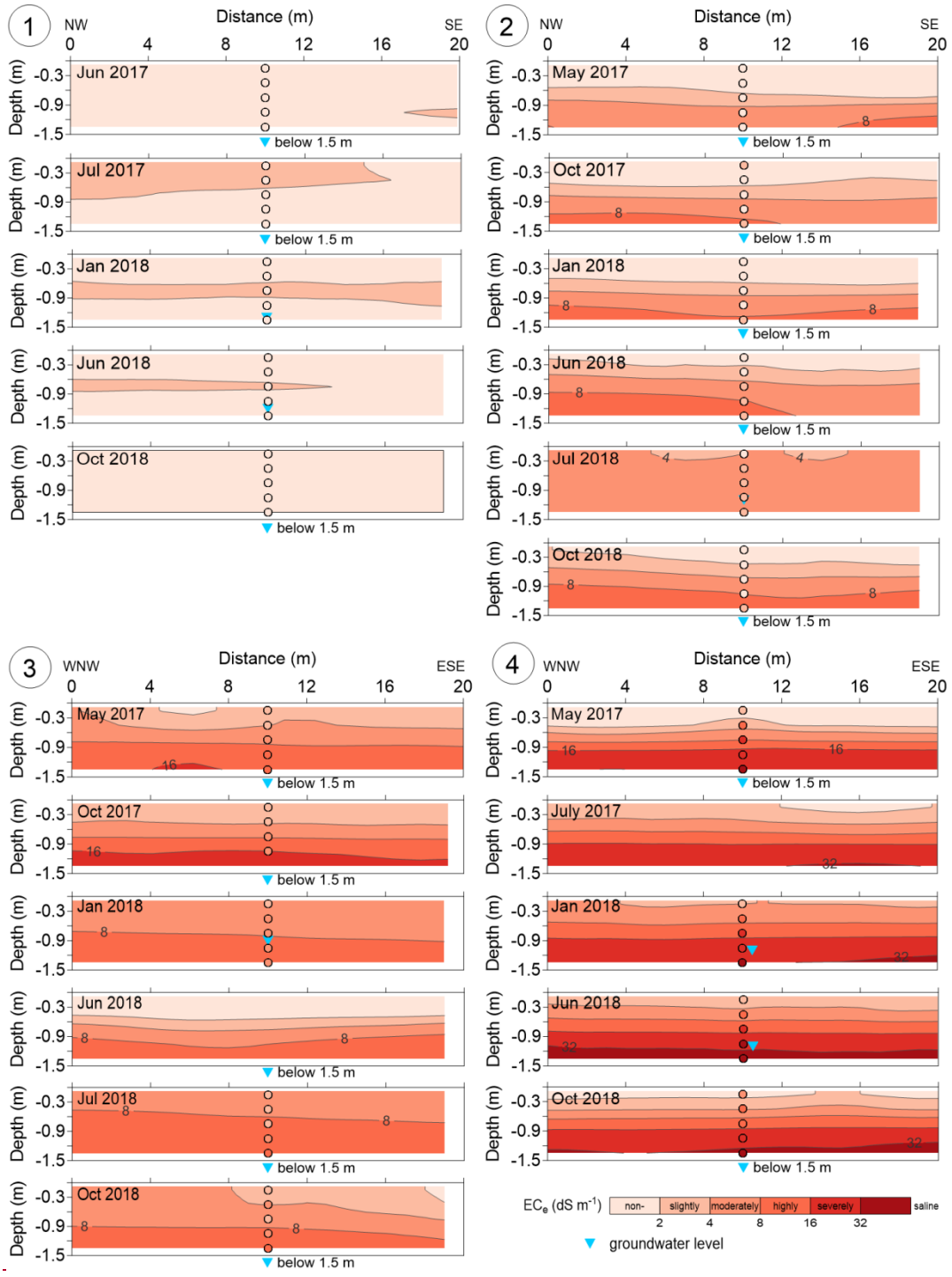

325 **Figure ~~5~~6: Cross sections~~Maps~~ of soil salinity (predicted EC_e) for locations 1 to 4, with representation of measured EC_e (in circles) and groundwater level (blue triangles) at the sampling sites located in the middle of each transect. Note that in June 2018 at location 3 and in July 2017 at location 4 there was no soil sampling.**

The salinity cross sections~~maps~~ for location 1 show that the soil is generally non-saline, with slightly saline zones in all dates except for October 2018. These saline zones occur in the top soil layers until 0.9 m depth (topsoil, subsurface and upper subsoil), and represent an overestimation of the soil salinity when compared to the measured EC_e of the sampling point (which is invariably non-saline). This overestimation tendency is in agreement with Fig. ~~4d~~5d, where the very low range of spatiotemporal variations of soil salinity at this location can also be observed. In such conditions, other soil properties, such as θ, dominate the small variations of σ, and therefore the ability to predict salinity from σ at this location was reduced. Our previous studies with both location-specific and regional calibrations tested at this location showed similar results (Farzamian et al., 2019).

At location 2 the salinity cross sections~~maps~~ show an increase of salinity with depth from non-saline at the topsoil to highly-saline in the lower subsoil, with exception of July 2018, where the entire soil profile is moderately saline. The increase of soil salinity in upper soil layers in July 2018 can be attributed to fertigation practices for the maize cultivation that introduced salts into the soil profile. The salinity cross sections~~maps~~ also show the overestimation of salinity occurring mainly at deeper soil layers, which agrees with the results presented in Fig. ~~4d~~ 5d and discussed in section 4.3~~2~~.

At location 3 soil salinity is well predicted in May 2017 but tends to be slightly overestimated in the remaining dates, especially in July 2018. The salinity cross sections~~maps~~ show that salinity increases with depth reaching severely-saline in May 2017 and October 2017. This can be due to the influence of the saline groundwater (as seen in Fig. 3, the intermediate and lower subsoil layers are permanently saturated). The groundwater level is above 1.5 m in January 2018, although the salinity of the deeper soil layers (>0.9 m) decreases compared to May and October 2017, which could be due to washing of the profile by rainfall. The increase of soil salinity in upper soil layers in July 2018, similarly to location 2 on the same date, can be attributed to fertigation practices for the maize cultivation.

At location 4 the trend of increasing salinity with depth is accurate in all dates, but it tends to be slightly underestimated. The salinity cross sections~~maps~~ show that salinity increases from non-saline in topsoil to severely-saline in lower subsoil. This is probably related to the saline groundwater level above 1.5 m. During the dry period of the year, salinity of the lower subsoil reaches the highest values (June 2018).

Comparison of the salinity cross sections~~maps~~ between locations confirms the previously known north-south soil salinity spatial gradient of the study area, that is, from location 1 to 4, soil salinity generally increases. Soil salinity dynamics at each location reveals fluctuations in time related to the input of salts and water either through irrigation, precipitation or groundwater level and salinity. Location 1 tends to have non-saline characteristics, which can be attributed to good quality irrigation~~-~~. In addition, ~~water and to the fact that~~ this location is far from the estuary, making it less prone to the presence of saline groundwater. At locations 2 and 3, the salinity ~~maps~~ cross sections show an increase of soil salinity in the upper layers during the dry season (when irrigation occurs), which decreases in the following months with increased rainfall (Fig. 2). At the rainfed location 4, it is also visible an increment of salinity along the entire profile during the dry season. This is likely due to the influence of the saline groundwater and capillary rise along the profile.

5 Conclusions

In this study, EMI and soil sampling data collected between May 2017 and October 2018 were used, together with a previously developed regional calibration, to predict soil salinity. This procedure allowed further validation of the regional calibration with an independent dataset and a preliminary qualitative analysis of soil salinity dynamics in the study area. Based on the comprehensive analysis of the statistical indicators obtained from the validation process, and the obtained soil salinity cross sections, the following main conclusions can be drawn:

1. The validation performed in this study resulted in a RMSE of 3.14 dS m^{-1}, which is acceptable given the large range of EC_e (52.35 dS m^{-1}). This validation resulted in lower prediction ability than that previously resulting from cross-validation. This is because the test set was independent, and also because it was collected over a wider period of time, with a larger variation of soil properties. In addition, prediction ability of the regional calibration does not vary significantly over time. As a result, the regional calibration approach still stands as an expeditious method to predict soil salinity from EMI surveys at any new location in the study area. However, prediction ability of the regional calibration in assessing variability of soil salinity at different locations and depths varies significantly due to variability of soil properties at each location and depth. Our investigation shows that significantly larger variations of EC_e and σ at location 4 dominated the regional regression calibration, suggesting a good prediction ability of the regional calibration in the south of the study area and close to location 4 where the soil salinization is of major concern and can compromise agricultural activity.
2. The methodology used in this study allowed the generation of soil salinity cross sections displaying the patterns of soil salinity at different dates, at four locations in the study area. The salinity cross sections show a qualitative response of soil salinity to the input of salts and water either through irrigation, precipitation or level and salinity

of groundwater. In a regional perspective, soil salinity dynamics in the study area may be preliminarily explained by a combination of spatial distribution of the marine fraction of soil, with irrigation practices in the study area and saline groundwater in the southern part.

Application of time-lapse EMCI and calibration for assessing soil salinity dynamics is a developing methodology that can further support the evaluation and adoption of proper agricultural management strategies in irrigated regions. Some aspects can and will be addressed in future studies so to improve its performance. From this study, we identify some of these aspects. First, relatively to the inversion process, and in the absence of a time-lapse inversion algorithm, EC_a data was inverted independently. This method can distort the inversion results, since the reference model and a priori information are not considered. Further research involves time-lapse inversion algorithms that are being developed to invert data collected with EMI sensors, which can generate EMCIs of higher precision. Secondly, the influence of static soil properties (i.e., that do not vary in time), such as clay content and cation exchange capacity, could be tackled with the use of cross sections of the variation of soil salinity between two consecutive dates, which allows removing the static effect from the time-lapse EMCIs. Finally, temporal soil salinity assessment can be optimized by quantitatively taking into account the influence of soil dynamic properties on the time-lapse EMCIs. Specifically, in Lezíria, regional calibrations can be improved by studying new locations across the study area for a longer period of time with more frequent surveying and sampling, and also by including new parameters, such as θ, soil temperature, level and salinity of groundwater. However, the temporal variations of these properties are connected to location specific conditions. For instance, θ can vary significantly in the study area, particularly in the root zone, due to different irrigation practices, rootup take of different crops, and fluctuation of groundwater level. These facts highlight the necessity of using location-specific calibrations for a more precise assessment of soil salinity changes at each location.~~In this study, EMI and soil sampling data collected between May 2017 and October 2018 were used, together with a previously developed regional calibration, to predict the spatiotemporal variability of soil salinity. This procedure allowed to further validate the regional calibration with an independent test set. This validation resulted in lower prediction ability than that previously resulting from cross-validation, not only because the test set was independent, but also because it was collected over a wider period of time, during which the variation of soil properties is larger. The validation used in this study resulted in a RMSE of 3.22 dS m^{-1}, which is acceptable given the large range of EC_e (52.35 dS m^{-1}). As a result, the regional calibration approach still stands as an expeditious method to predict soil salinity in the study area over~~

~~time. The regional calibration could be further developed by studying new locations across the study area in order to include a wider range of variation of soil properties. Also, a longer period of observation could further improve the regional calibration. Furthermore, the influence of static soil properties (i.e., that do not vary in time), such as clay content, could be tackled with the use of maps of the variation of soil salinity between two consecutive dates, which allows removing the static effect in the EMCIs.~~

~~Relatively to the inversion process, in the absence of a time-lapse inversion algorithm, EC_a data was inverted independently. This method can distort the inversion results, since the reference model and a priori information are not considered. Further research involves time lapse inversion algorithms that are being developed to invert data collected with EMI sensors, which can generate EMCIs of higher precision.~~

~~The methodology used in this study allowed the creation of soil salinity maps displaying the spatiotemporal patterns of soil salinity at four locations in the study area. The salinity maps reveal fluctuations in time related to the input of salts and water either through irrigation, precipitation or groundwater level and salinity.In a regional perspective, soil salinity dynamics in the study area may be explained by a combination of spatial distribution of the marine fraction of soil, with irrigation practices in the study area and saline groundwater in the southern part. Continuous monitoring of salinity in the study area, along with detailed data collection about irrigation, precipitation, evapotranspiration, leaching, groundwater flow, and tides, can be helpful to further study soil salinity dynamics.~~

~~Time lapse EMCI has proven to be a valid methodology for evaluating risk of soil salinization, and can further support the evaluation and adoption of proper agricultural management strategies, especially in irrigated areas, where continuous monitoring of soil salinity dynamicsis required.~~

Acknowledgements

The authors are grateful to the Associação de Beneficiários da Lezíria Grande de Vila Franca de Xira and to Manuel Fernandes and Fernando Pires from INIAV for field assistance.

This work was funded by the Portuguese research agency, Fundação para a Ciência e a Tecnologia (FCT), in the scope of project SALTFREE – ARIMNET2/0004/2015 SALTFREE and ARIMNET2/0005/2015 SALTFREE. Publication is supported by FCT – project UID/GEO/50019/2019 – Instituto Dom Luiz.

References

Barrett-Lennard, E. G., Bennett, S. J., and Colmer, T. D.: Standardising the terminology for describing the level of salinity in soils. In: Proceedings of the 2nd international salinity forum: Salinity, water and society global issues, local action, Adelaide, SA, Australia, 31 Mar.–3 Apr. 2008. Geological Society of Australia, Hornsby, NSW, Australia, 2008.

Bouksila, F., Persson, M., Bahri, A., and Berndtsson, R.: Electromagnetic inductionprediction of soil salinity and groundwater properties in a Tunisian Saharan oasis. Hydrol. Sci. J., 57, 1473–1486, https://doi.org/10.1080/02626667.2012.717701, 2012.

Corwin, D.L. and Lesch, S.M.: Characterizing soil spatial variability with apparent soilelectrical conductivity: I. Survey protocols. Comp. Elec. Agri. Appl. Apparent Soil Elec. Conductivity Precis. Agri., 46, 103–133, https://doi.org/10.1016/j.compag.2004.11.002, 2005.

Corwin, D.L. and Scudiero, E.: Chapter One - Review of soil salinity assessment for agriculture across multiple scales using proximal and/or remote sensors. Adv Agron, 158, 1–130, https://doi.org/10.1016/bs.agron.2019.07.001, 2019.

Dafflon, B., Hubbard, S., Ulrich, C., and Peterson, J.E.: Electrical conductivity imaging of active layer and permafrost in an arctic ecosystem, through advanced inversion of electromagnetic induction data. Vadose Zone J., 12, https://doi.org/10.2136/vzj2012.0161, 2013.

De Groot-Hedlin, C. and Constable, S.C.: Occam's inversion to generate smooth, two dimensional models from magnetotelluric data. Geophysics, 55, 1613–1624, https://doi.org/10.1190/1.1442813, 1990.

Farzamian, M., Monteiro Santos, F. A., and Khalil, A.M.: Application of EM38 and ERT methods in estimation of saturated hydraulic conductivity in unsaturated soil. J. Appl. Geophys., 112, 175–189, https://doi.org/10.1016/j.jappgeo.2014.11.016, 2015.

Farzamian, M., Paz, M.C., Paz, A.M., Castanheira, N.L., Gonçalves, M.C., Santos, F.A.M., and Triantafilis, J.: Mapping soil salinity using electromagnetic conductivity imaging-a comparison of regional and location-specific calibrations. Land Degrad. Dev., 30, 1393–1406, https://doi.org/10.1002/ldr.3317, 2019.

Fischer, G., Nachtergaele, F.O., Prieler, S., Teixeira, E., Toth, G., van Velthuizen, H., Verelst, L., and Wiberg, D.: Global Agro-ecological Zones (GAEZ v3.0)-Model Documentation [WWW Document]. URL http://www.fao.org/soils-portal/soil-survey/soil-maps-and-databases/harmonized-world-soil-database-v12/en/ (accessed 12.17.18), 2012.

Huang, J., Purushothaman, R., McBratney, A., and Bramley, H.: Soil water extraction monitored per plot across a field experiment using repeated electromagnetic induction surveys. Soil Syst., 2(1), 11, https://doi.org/10.3390/soilsystems2010011, 2018.

Huang, J., Scudiero, E., Clary, W., Corwin, D. L., and Triantafilis, J.: Time-lapse monitoring of soil water content using electromagnetic conductivity imaging. Soil Use Manage., 33, https://doi.org/10.1111/sum.12261, 2017.

Jadoon, K.Z., Moghadas, D., Jadoon, A., Missimer, T.M., Al-Mashharawi, S.K., and McCabe, M.F.: Estimation of soil salinity in a drip irrigation system by using joint inversion of multicoil electromagnetic induction measurements. Water Resour. Res., 51, 3490–3504, https://doi.org/10.1002/2014WR016245, 2015.

Kaufman, A.A. and Keller, G.V.: Frequency and transient soundings. Methods in Geochemistry and Geophysics, 16. Elsevier, New York, https://doi.org/10.1111/j.1365-246X.1984.tb02230.x, 1983.

Kaufmann, M.S.; von Hebel, C.; Weihermüller, L.; Baumecker, M.; Döring, T.; Schweitzer, K.; Hobley, E.; Bauke, S.L.; Amelung, W.; Vereecken, H.; et al. Effect of fertilizers and irrigation on multi-configuration electromagnetic induction measurements. Soil Use Manage., 36, https://doi.org/10.1111/sum.12530, 2019.

Lin, L. I. K.: A concordance correlation coefficient to evaluate reproducibility. Biometrics, 45, 255–268, https://doi.org/10.2136/sssaj1998.03615995006200010030x, 1989.

Moghadas, D., Jadoon, K.Z., and McCabe., M.F.: Spatiotemporal monitoring of soil water content profiles in an irrigated field using probabilistic inversion of time-lapse EMI data. Adv. Water Resour., 110, 238–248, https://doi.org/10.1016/j.advwatres.2017.10.019, 2017.

Monteiro Santos, F.A.: 1-D laterally constrained inversion of EM34 profiling data. J. Appl. Geophys., 56, 123–134, https://doi.org/10.1016/j.jappgeo.2004.04.005, 2004.

Monteiro Santos, F.A., Triantafilis, J., and Bruzgulis, K.: A spatially constrained 1D inversion algorithm for quasi-3D conductivity imaging: application to DUALEM-421 data collected in a riverine plain. Geophysics, 76, B43–B53, https://doi.org/10.1190/1.3537834., 2011.

Paz, A., Castanheira., N., Farzamian, M., Paz, M.C., Gonçalves, M., Monteiro Santos, F., and Triantafilis, J.: Prediction of soil salinity and sodicity using electromagnetic conductivity imaging. Geoderma, 361, https://doi.org/10.1016/j.geoderma.2019.114086, ~~*in press*~~, 2019a.

Paz, M.C., Farzamian, M., Monteiro Santos, F., Gonçalves, M.C., Paz, A.M., Castanheira., N.L., and Triantafilis, J.: Potential to map soil salinity using inversion modelling of EM38 sensor data. First Break, 37(6), 35–39, doi:10.3997/1365-2397.2019019, 2019b.

Richards, L.A. (Ed.), 1954. Diagnosis and Improvement of Saline and Alkali Soils. Agricultural Handbook, USDA.

Shanahan, P.W., Binley, A., Whalley, W.R., and Watts., C.W.: The use of electromagnetic induction to monitor changes in soil moisture profiles beneath different wheat genotypes. Soil Sci. Soc. Am. J., 79, 459–466, https://doi.org/10.2136/sssaj2014.09.0360, 2015.

Triantafilis. J., Laslett, G.M., andMcBratney, A.B.: Calibrating an electromagnetic induction instrument to measure salinity in soil under irrigated cotton. Soil Sci. Soc. Am. J., 64, 1008-1017, https://doi.org/10.2136/sssaj2000.6431009x, 2000.

Triantafilis, J., Odeh, I.O.A.V., and McBratney, A.B.: Five geostatistical methods to predict soil salinity from electromagnetic induction data across irrigated cotton. Soil Sci. Soc. Am. J., 65, 869-978, https://doi.org/10.2136/sssaj2001.653869x, 2001.

Triantafilis, J. and Monteiro Santos, F.A.: 2-dimensional soil and vadose zone representation using an EM38 and EM34 and a laterally constrained inversion model. Aust. J. Soil Res., 47, 809–820,https://doi.org/10.1071/SR09013, 2009.

von Hebel, C., van der Kruk, J., Huisman, J.A., Mester, A., Altdorff, D., Endres, A.L., Zimmermann, E., Garré, S., and Vereecken, H.: Calibration, Conversion, and QuantitativeMulti-Layer Inversion of Multi-Coil Rigid-Boom Electromagnetic Induction. Sensors, 19, 4753, https://doi.org/10.3390/s19214753, 2019.

von Hebel, C., Rudolph, S., Mester, A., Huisman, J.A., Kumbhar, P., Vereecken, H., and van der Kruk, J.: Three-dimensional imaging of subsurface structural patterns using quantitative large-scale multi-configuration electromagnetic induction data. Water Resour. Res., 50, 2732–2748, https://doi.org/10.1002/2013wr014864, 2014.